Geomagnetic Paleointensities From Radiocarbon-Dated Lava Flows on Hawaii and the Question of the Pacific Nondipole Low

ROBERT S. COE

Earth Sciences Board, University of California, Santa Cruz, California 95064
U.S. Geological Survey, Menlo Park, California 94025

SHERMAN GROMMÉ AND EDWARD A. MANKINEN

U.S. Geological Survey, Menlo Park, California 94025

Radiocarbon ages have been published for nine basaltic lava flows on the island of Hawaii; the ages range from 2600 to somewhat older than 17,900 years B.P. By using the Thelliers' method in vacuum, geomagnetic paleointensity values were obtained from eight of the lavas; the ninth proved unsuitable. The paleointensities for the four youngest flows (2600–4600 years B.P.) yield virtual dipole moments (VDM's) that are 20% greater to more than twice the worldwide values for those times obtained by V. Bucha from archeomagnetic data. The dispersion of virtual geomagnetic poles for the eight lavas is 15.5°, appreciably larger than the average for older lava flows on Hawaii. These results contrast with the historic magnetic field in the region of Hawaii, in which both secular variation and nondipole components are very low. At about 10,000 years B.P. the measured VDM is not very different from the long-term worldwide average but differs considerably from a smooth extrapolation of Bucha's average curve. At about 18,000 years B.P. the measured VDM is very low and is associated with an unusually shallow paleomagnetic inclination for the latitude of Hawaii. These new paleointensity and paleodirectional data strongly suggest that sizable nondipole geomagnetic fields have existed in the vicinity of Hawaii at various times during the Holocene epoch and perhaps earlier.

INTRODUCTION

Considerable paleomagnetic evidence from the island of Hawaii has been amassed in support of the hypothesis that the central Pacific has been a region of very low nondipole field for the past 0.7 m.y. or more [*Cox and Doell,* 1964; *Doell and Cox,* 1965, 1971, 1972]. The suggested explanation of lateral variation of temperature or topography of the core-mantle boundary has provoked a considerable amount of wide ranging speculation [*Cox and Cain,* 1972]. Recently, various aspects of this hypothesis have been called into question [*Duncan,* 1975; *McElhinny and Merrill,* 1975], and *Cox* [1975] himself has reinterpreted the inclination variations in the Hawaiian paleomagnetic data as implying the presence of significant components of the drifting part of the nondipole field.

The arguments for and against the hypothesis are complex and depend on a variety of assumptions. Most investigations of the nondipole field by paleomagnetic means are frustratingly indeterminate because the dipole field is usually not well enough known to permit identification of the nondipole component of the ancient field. Instead, what is done is to characterize the paleomagnetic secular variation at a restricted locality over some period of time by means of the angular standard deviation of field directions or virtual geomagnetic poles and to make assumptions regarding the wobble and change of moment of the dipole field. The main evidence that the present low nondipole field has been a persistent feature of the past 0.7 m.y. or more is the low secular variation suggested by extensive paleomagnetic studies in the Hawaiian Islands [*Doell and Cox,* 1965, 1971, 1972; *Doell,* 1969]. The difficulty with this inference is that sequences of lava flows give a discontinuous and irregular record of the ancient field with time, so significant changes of the nondipole field may have been missed or incompletely sampled [*McElhinny and Merrill,* 1975].

Another problem with most paleomagnetic studies of secular variation is that the intensity of the ancient field is not determined. One must rely entirely on the variation of field directions, which means that in addition to assumptions regarding the dipole field, another assumption about the direction of the nondipole field vector is required to separate the dipole and nondipole components. The usual assumption has been that the nondipole field vectors are randomly oriented when they are sampled over a sufficient length of time, but it now seems likely that this is seriously in error [*Cox,* 1975].

Maps of the nondipole field as long ago as 1650 A.D. have been constructed by *Yukutake and Tachinaka* [1968], using spherical harmonic analysis. Large nondipole fields in the central Pacific are shown in their maps for 1650 and 1700, but these must be regarded as questionable, since they are based on few data. *Doell and Cox* [1972] consider the first reliable analysis given by Yukutake and Tachinaka to be that for 1829, and the maps for this year and all subsequent years show very low nondipole fields in the central Pacific. One hundred and fifty years, however, is much too short a time to provide much support for the hypothesis that the nondipole field has been low there for the past 0.7 m.y.

The opportunity exists to extend greatly by paleomagnetic means observations of the nondipole field because the variation of the geomagnetic dipole moment has been delineated, at least roughly, for the past 8500 years by archeomagnetic studies, summarized by *Cox* [1968] and *Bucha* [1970, 1971]. With this in mind we collected for paleointensity studies all the radiocarbon-dated basalt flows that we could find on the island of Hawaii. Our thought was that if results from the samples a few thousand years in age confirmed the hypothesis of low nondipole field in the central Pacific, then older samples could possibly be used to extend the record of dipole moment further into the past without the need for simultaneous measurements at many points in the globe. Our results, however, do not confirm this hypothesis but point instead to the exis-

Paper number 7B1131.
0148-0227/78/047B-1131$03.00

TABLE 1. Paleomagnetic Directional Data, Dated Holocene Hawaiian Lavas

Flow Name and Source	Age, yr	Reference	*SLA*, deg	*SLO*, deg	N/N_0	$\bar{H}$, Oe	k	α_{95}, deg	I, deg	D, deg	*PLA*, deg	*PLO*, deg
Visitor Center, K	≥2570 ± 250	*Rubin and Suess* [1956], *Powers* [1948, 1955]	19.433	204.744	9/9	0	812	1.8	41.4	3.4	84.6	240.1
Waiohinu, ML	3850 ± 250 3720 ± 250	*Rubin and Alexander* [1960] *Sullivan et al.* [1970]	19.071	204.386	2/2*	0	...	...	27.4	21.0	69.4	303.9
Puu Loa Loa, MK	870–4530	*Porter* [1971]	19.718	204.561	8/8	50	181	4.1	46.0	4.7	81.2	233.0
Puu Kole, MK	4530 ± 110	*Porter* [1971]	19.731	204.590	6/8	150	330	3.7	41.5	19.7	71.3	278.2
Hale Pohaku, MK	4600 ± 190	*Porter* [1971]	19.729	204.575	8/8	0	174	4.2	27.5	21.3	69.0	305.4
Maniania Pali I, ML	10,410 ± 310	*Rubin and Berthold* [1961]	19.047	204.449	8/9	100	857	1.9	49.4	27.4	62.8	264.8
Maniania Pali II, ML	>10,410	*Rubin and Berthold* [1961]	19.047	204.449	7/9	100	59	8.0	1.1	353.2	70.3	45.1
Hilina Pali I, K	17,860 ± 670	*Rubin and Berthold* [1961]	19.272	204.714	6/6	50	232	4.4	8.5	7.9	73.1	356.5
Hilina Pali II, K	>17,860	*Rubin and Berthold* [1961]	19.272	204.714	0†	...	...	...	...	...	...	...

Sources are K, Kilauea; ML, Mauna Loa; MK, Mauna Kea. Age is uncorrected radiocarbon years before present, using 5730-year half life for ^{14}C. *SLA* and *SLO* are north latitude and east longitude of sampling site. N/N_0 is number of oriented samples accepted per number measured. $\bar{H}$ is peak alternating demagnetizing field. Parameters k and α_{95} are precision parameter and radius of 95% confidence cone [*Fisher*, 1953]. I and D are inclination downward and declination eastward of mean remanent magnetization direction. *PLA* and *PLO* are north latitude and east longitude of virtual geomagnetic pole.

*Two specimens from a single oriented hand sample.

†Unoriented hand sample.

tence of a rather large nondipole geomagnetic field in Hawaii in the recent past.

In the first part of this paper we present new paleomagnetic data from nine radiocarbon-dated basalts from the island of Hawaii: in addition to the usual directional information we have determined paleointensities using the double-heating method [*Thellier and Thellier*, 1959]. By comparing the data for three of the younger flows with worldwide average values of the earth's dipole moment we are able to estimate both the direction and the intensity of a rather strong nondipole field at Hawaii at the times that these lavas were erupted. In the second part of the paper we reevaluate the magnitude of Brunhes epoch secular variation from the large quantity of data on paleomagnetic directions for the Hawaiian Islands published heretofore and conclude that the low value published by *Doell and Cox* [1971, 1972] may be too low because many of the data may have been obtained from lavas erupted in rapid succession. Because both the directions and the intensities of the magnetic field that we obtained from the radiocarbon-dated lavas are very different from what would be predicted if only the dipole field had been present at Hawaii, we conclude that a low in the nondipole field at Hawaii throughout Holocene time is unlikely.

SAMPLES

We collected samples from nine young basalt flows on the island of Hawaii. Three were erupted from the volcano Kilauea, three from Mauna Loa, and three from Mauna Kea. Their informal names, the volcano from which they issued, their geographic coordinates, and their estimated ages are given in Table 1. Radiocarbon dating provides reasonably precise ages for six of the flows, minimum ages for two of the flows (Maniania Pali II and Hilina Pali II) that underlie the respective dated flows, and upper and lower bounds for the age of the remaining flow (Puu Loa Loa). The age of the Visitor Center flow requires a little discussion: The dated material was charcoal from a fern mold in pumice overlying the lava [*Rubin and Suess*, 1956]. From the discussions of *Powers* [1948, 1955] concerning rates of accumulation and soil formation for these rocks (the Puna volcanic series) we estimate that the actual age of the lava flow lies within the ±250-year uncertainty of the minimum age of 2570 B.P.

We drilled and oriented a minimum of six cores from seven of the flows using a portable gasoline-powered diamond drill. From one of the remaining flows we took one oriented and one unoriented hand sample, and from the other only an unoriented hand sample (Table 1). Overall orientation errors are 2°–3° for the cores and about 7° for the hand sample.

PALEOMAGNETIC DIRECTIONS

We measured the directions of natural remanent magnetization (NRM) of the oriented specimens with a spinner magnetometer and cleaned them in alternating fields at 60 Hz in a demagnetizing device with a four-axis tumbler; af cleaning was not necessary for three of these very young flows, and in general, we obtained high-quality results. All results are given in Table 1.

The virtual geomagnetic poles (VGP's) corresponding to the directions of NRM of the eight flows for which we collected oriented samples do not cluster around the geographic pole (Figure 1). Rather, the average pole lies about 9° to the right side as viewed from Hawaii, very near the present inclined dipole and the mean historic VGP for Hawaii. Discussion of the dispersion of the VGP's shown in Figure 1 and its significance for estimating secular variation is deferred to a later section.

PALEOINTENSITIES

Experiments

We selected for study those samples from each flow whose directions lay close to the af-cleaned mean direction for the flow. Excluding those with anomalously high strengths of NRM, we took the remainder to be the most likely to be free of large secondary components of magnetization. On portions of these we conducted tests on strong-field magnetization J_s versus temperature T in a vacuum of about 2×10^{-4} torr with an automatic recording magnetic balance in fields of a few kilooersteds. The J_s-T tests provide information concerning changes in magnetic properties of the rock during heating and, by the Curie points obtained, serve as a rough guide in choosing temperature steps in the subsequent paleointensity experiments.

The method that we use to determine ancient field intensities is that developed by *Thellier and Thellier* [1959], demonstrated to be better than several others for basalts [*Coe and Grommé*,

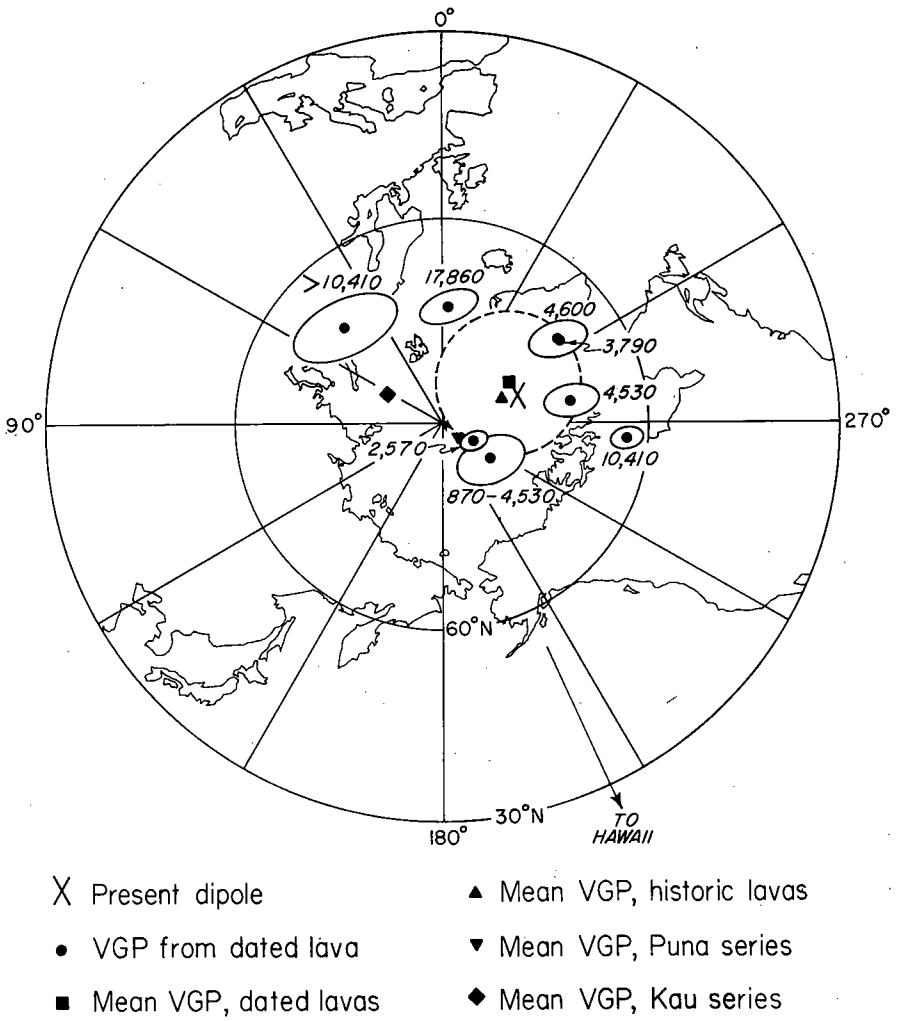

Fig. 1. Equal-area projection of part of northern hemisphere showing VGP's from ^{14}C-dated Hawaiian lavas with corresponding ages in years B.P., the present geomagnetic dipole, and mean VGP's from Hawaiian historic, ^{14}C-dated, Puna series, and Kau series lavas. For the ^{14}C-dated lavas, 95% confidence ovals for individual VGP's are shown as solid lines; the 95% confidence circle for the mean is shown dashed; 95% confidence circles for the other lava series are smaller than the plotted symbols. Data are from Tables 1 and 5. Radiocarbon ages are calculated with 5730-year half life.

1973]. The reason is that in the Thelliers' method the specimen is subjected to a series of pairs of heating experiments that progress from room temperature to higher temperatures, the progression thereby permitting the collection of useful intensity information at low temperatures before the occurrence at higher temperatures of alterations of magnetic mineralogy such as oxidation, reduction, etc. At each step of the series the specimen is heated twice to the same temperature T_i and cooled in different magnetic fields. Measuring the remanence after cooling makes possible the determination of both the NRM that remains with blocking temperatures $T_b > T_i$ and the thermoremanent magnetization (TRM) that is acquired with T_b between T_i and room temperature T_r. In the variant of the Thelliers' method that we use [*Coe*, 1967*a*, *b*], the field is zero during the first heating and cooling cycle of the pair and some small (0.4 Oe in this study) but nonzero value during the second. Comparison of the spectra of the NRM and artificial TRM then yields an estimate of the paleointensity. All these experiments were done in a vacuum of about 1×10^{-5} torr, and complete heating-cooling cycles were several hours long [*Khodair and Coe*, 1975].

The clearest way to present such data is in terms of an NRM-TRM diagram [*Arai*, 1963; *Nagata et al.*, 1963] in which the NRM (y_i) remaining at each temperature step T_i is plotted against the corresponding TRM (x_i) acquired. Ideally, these points will fall on a straight line whose slope is determined by the ratio of the intensity of the ancient earth's magnetic field F_E to that of the laboratory field F_L:

$$y = a - (F_E/F_L)x \qquad (1)$$

We have developed criteria and statistical methods for the analysis of NRM-TRM curves, and these are presented in the appendix.

Results

The results of the intensity experiments and their analysis are contained in Table 2 in a very compressed format. A few illustrative examples may help the reader interpret their significance. For details concerning definitions of quality factor q, NRM fraction f, and gap factor g, refer to the appendix.

Sample 142 of the Waiohinu flow (3740 years B.P.) yielded a high-quality (q = 40.1) paleointensity of 0.514 Oe. Figure 2*a* shows the NRM-TRM curve. The least squares segment is defined quite well by 13 points between 20° and 351°C that span 88.3% of the total NRM, and there are four rather checks. (See the appendix for a description of PTRM

TABLE 2. Strong-Field Measurements and Paleomagnetic Intensity Data

Flow Name	Specimen	T_c, °C	T_c', °C	J_s'/J_s	ΔT, °C	N	f	g	σ_b/b	q	F_E	$\bar{F}_E \pm \sigma_{\bar{F}}$	VDM $\pm \sigma_{\bar{v}}$, $\times 10^{25}$ emu cm^3
Visitor	184	530	520	0.93	149–502	10	0.405	0.790	0.0207	15.5	0.601		
Center	186	(250), 550	570	0.91	20–522	16	0.618	0.898	0.0341	16.3	0.517	0.580 ± 0.029	12.34 ± 0.62
	190	535	525	0.93	148–521	12	0.588	0.839	0.0185	26.7	0.605		
Waiohinu	141	250, 570	280, 570	0.97	20–342	13	0.740	0.890	0.0123	53.7	0.564	0.548 ± 0.027	13.04 ± 0.64
	142	180, (490)	180, (490)	0.99	20–351	13	0.88	0.872	0.0192	40.1	0.514		
Puu Loa	113	155, (545)	155,(545)	1.00	80–320	13	0.725	0.899	0.0219	29.8	0.572		
Loa	114	155, (550)	160, (550)	0.99	59–226	9	0.551	0.837	0.0440	10.5	0.506	0.560 ± 0.048	11.39 ± 0.98
	117	155, 575	160, 575	1.02	20–153	7	0.414	0.785	0.0711	4.6	0.456		
Puu	123	(~280), 545	(~280), 545	0.96	...	...	...	...	...	...	...		
Kole	124	550	550	0.95	...	...	...	...	...	...	...	...	...
	127	540	530	0.95	...	...	...	...	...	...	...		
Hale	132	150, 550	190, 550	0.91	98–346	6	0.300	0.781	0.0557	4.2	0.500		
Pohaku	133	190, 575	160, 575	0.94	20–350	13	0.348	0.901	0.0291	10.8	0.518	0.543 ± 0.050	12.92 ± 1.19
	137	190, 565	170, 565	0.93	20–251	10	0.414	0.868	0.0495	7.3	0.656		
Maniania	078	105, 575	125, 575	1.06	20–123	5	0.371	0.729	0.0410	6.6	0.407		
Pali I	080	225, 560	220, 540	0.97	20–348	7	0.361	0.824	0.0513	5.8	0.466	0.446 ± 0.018	8.72 ± 0.35
	082	190, 575	185, 570	1.04	20–124	5	0.431	0.721	0.0263	11.8	0.457		
	083*	170, 505	180, 505	1.03	...	...	...	...	...	...	...		
Maniania	086	?–520	250–520	0.94	81–249	8	0.361	0.813	0.0679	4.3	0.358		
Pali II	087*	570	570	1.00	20–550	12	0.916	0.586	0.0290	18.5	0.294	0.294 ± 0.035	7.60 ± 0.90
	092	255, 575	230, 575	0.93	20–344	7	0.193	0.825	0.0525	3.0	0.237		
	093	255, 565	240, 565	0.93	95–395	7	0.219	0.786	0.0770	2.2	0.263		
Hilina	094	~200	~170	0.89	121–196	4	0.230	0.641	0.0421	3.5	0.096		
Pali I	096	~220–540	220–540	0.94	98–345	6	0.225	0.793	0.0515	3.5	0.229	0.143 ± 0.040	3.68 ± 1.08
	100	515	515	0.96	207–577	11	0.977	0.859	0.0219	38.3	0.144		
	103*	520	510	1.04	...	...	...	...	...	...	...		
	105*	190, 495	280–500	0.97	...	...	...	...	...	...	...		
Hilina Pali II	019	550	550	0.92	20–600	18	0.993	0.829	0.0119	69.4	0.215	0.215	4.83†

T_c and T_c' are Curie temperatures during heating and cooling, respectively. Most samples have two distinct Curie temperatures; parentheses around one indicate that only a minor amount of that phase is present. Dash between values indicates that sample has continuously distributed Curie temperatures. J_s'/J_s is ratio of room temperature strong-field magnetizations after and before heating. ΔT and N are temperature range and number of NRM-TRM points used to determine paleointensity; f is fraction of total extrapolated NRM spanned by least squares line segment; g is gap factor for points defining least squares line segment; σ_b/b is relative standard deviation of slope of least squares line segment; and q is overall quality factor of individual paleointensity estimate. F_E is paleointensity estimate for individual specimen. $\bar{F}_E \pm \sigma_{\bar{F}}$ is weighted mean paleointensity plus or minus standard error of the mean. VDM $\pm \sigma_{\bar{v}}$ is weighted mean virtual dipole moment plus or minus standard error.

*Determinations by A. Khodair (written communication, 1976) in this laboratory.

†Calculated assuming axial dipole orientation.

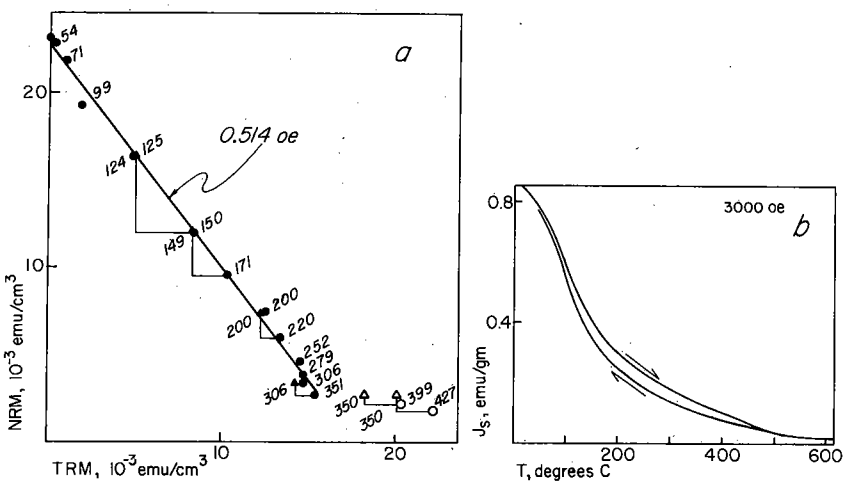

Fig. 2. (*a*) NRM-TRM diagram for specimen 142 (Table 3). Circles are NRM-TRM points, with temperatures in degrees Celsius shown to upper right; triangles are PTRM checks, with temperatures shown to lower left. Short straight line segments connect PTRM check points to the maximum temperature to which the sample was heated before doing the check; this is only the first, field-off heating of a pair (see text). NRM values for PTRM check points were obtained by linear interpolation between appropriate NRM-TRM points. Open symbols are rejected points; solid circles are points used to calculate the least squares line, shown as a solid line with paleointensity indicated. (*b*) Strong-field thermomagnetic curve for adjacent specimen from the same core, in vacuum, in the indicated field. Heating and cooling curves are designated by arrows; rates were 10°C per minute.

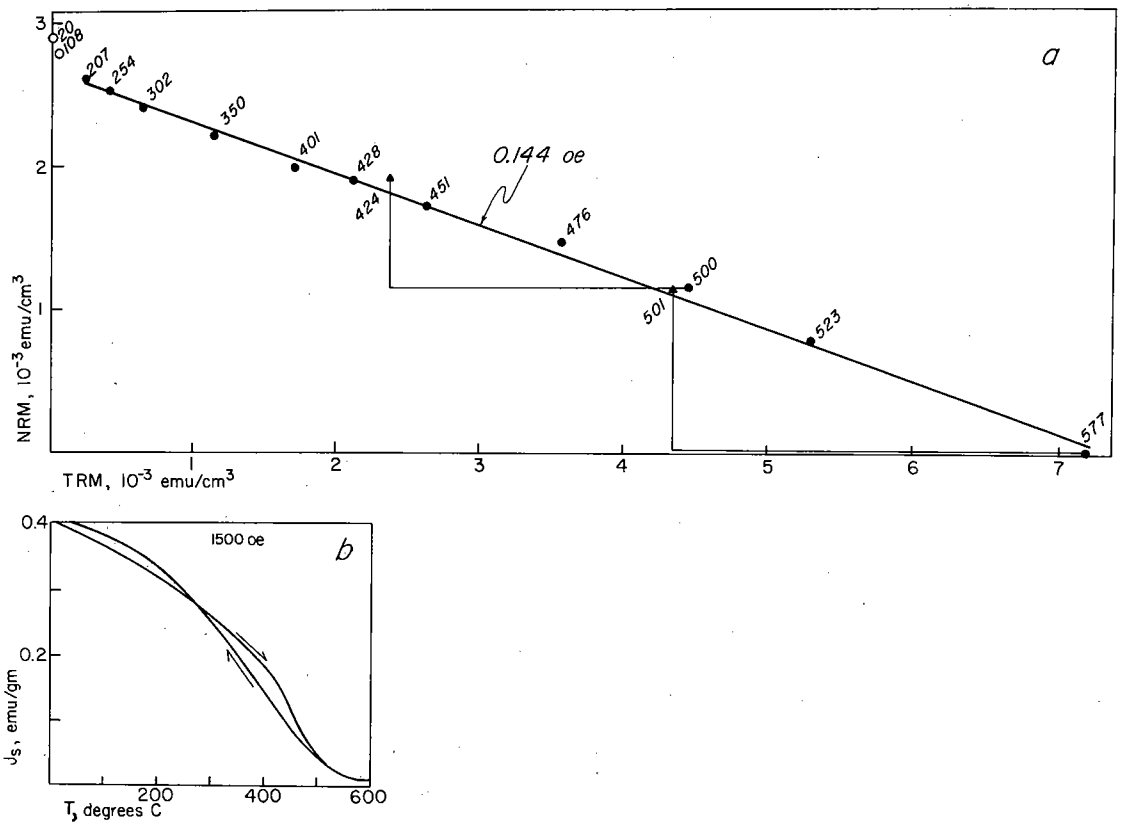

Fig. 3. (*a*) NRM-TRM diagram and (*b*) J_s-T curves for specimen 100. Symbols are as described in Figure 2.

checks.) The J_s-T heating and cooling curves are fairly similar and show that low Curie temperature phases predominate (Figure 2*b*). The other sample studied from this flow yielded a paleointensity of even higher quality in reasonably good agreement with this one (0.564 Oe). Moreover, studies of historic Hawaiian basalts erupted in known fields have demonstrated that reliable paleointensities can be obtained with encouraging consistency from unweathered, low Curie point basalts by the Thelliers' method in vacuum [*Khodair and Coe*, 1975]. On this evidence we believe that the mean field intensity for this flow of 0.548 ± 0.027 Oe is a figure in which we can have confidence, despite the fact that it is very high in comparison to the present intensity.

The other three examples are all from the Hilina Pali I flow (17,360 years B.P.) and illustrate the great range of magnetic behavior that may be encountered in a single flow. The NRM-TRM curve of sample 100 (Figure 3*a*) is very good; its overall quality factor is 38.3, and there are two consistent PTRM checks. The shallow slope corresponds to an unusually low paleointensity of 0.144 Oe. The initial steeper-sloped segment between 20° and 207°C is almost certainly due to viscous remanent magnetization (VRM). The J_s-T curve (Figure 3*b*) is reasonably regular and reversible and shows a high Curie temperature around 550°C.

Sample 096 alters during heating in the laboratory so as to increase its TRM capacity. This is indicated (Figure 4*a*) both

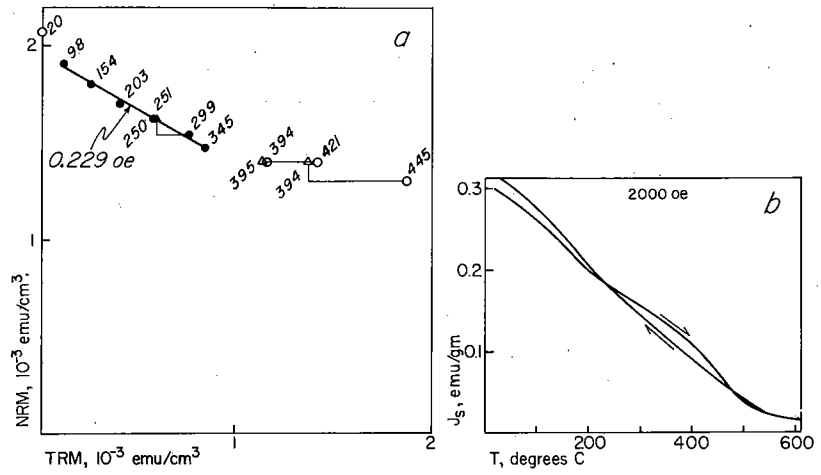

Fig. 4. (*a*) NRM-TRM diagram and (*b*) J_s-T curves for specimen 096. Symbols are as described in Figure 2.

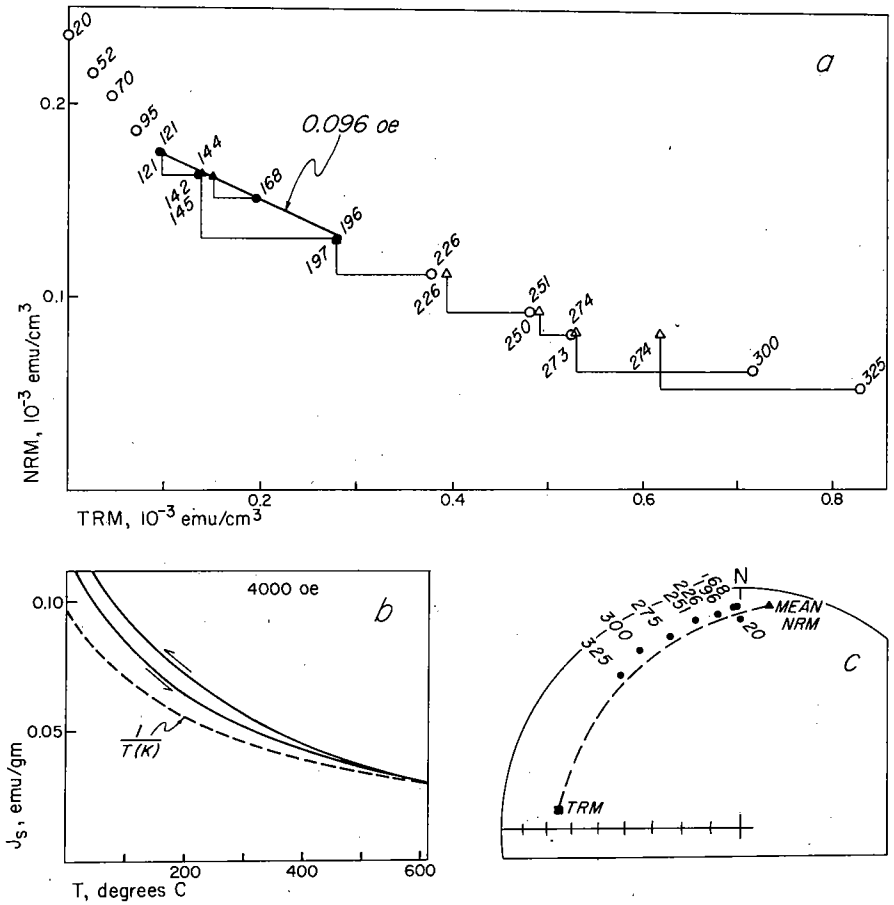

Fig. 5. (*a*) NRM-TRM diagram and (*b*) J_s-T curves for specimen 094. On Figure 5*b* a paramagnetic susceptibility curve is shown (dashed curve) for comparison, normalized to J_s of the sample at 610°C. (*c*) Lower hemisphere equal-area diagram of NRM directions during the Thelliers' experiment, in which temperatures correspond to Figure 5*a*, the TRM point is the direction of the applied field, and the NRM point is the mean direction for this lava flow after af demagnetization, in 50 Oe.

by the shape of the NRM-TRM curve and by the last two PTRM checks. The J_s-T curves (Figure 4*b*) show initially two indistinct Curie temperatures which become even more smoothly distributed after heating, although the heating and cooling curves do not depart from each other by a great deal. We interpret the VRM to be substantially removed by 98°C and the alteration to begin after 345°C, leaving a fairly straight segment containing only six points that defines a very low quality (q = 3.5) paleointensity of 0.229 Oe.

The final example, sample 094, is also far from ideal. Its NRM-TRM curve (Figure 5*a*) is not unlike the previous one, with a steep slope at low temperature due to VRM and ever shallowing slopes at higher temperatures due to alteration, but in this case there is a further subtlety. The apparent NRM direction moves toward that of the applied TRM at the higher temperature steps (Figure 5*c*), a situation showing that alteration during the field-on, TRM-producing cycle is also producing a component of chemical remanent magnetization (CRM) with even higher blocking temperatures parallel to the TRM that is persisting in part to the next (field-off) cycle. This sample is much harder to saturate than the other two and has a much lower J_s and NRM, and it probably has a large superparamagnetic fraction because its J_s-T curve is quite similar to the $1/T$ form of curve characteristic of paramagnetism (Figure 5*b*). This sample was obtained from the base of the lava flow, 5 cm above the lower contact, and apparently had been chilled very rapidly. It may be that the titanomagnetite in this sample is much finer grained than that in the other two and has partially altered to titanomaghemite during weathering. During heating, whether in air or in vacuum, this would disproportionate to yield magnetite [*Ozima and Ozima,* 1971]; thus J_s would be increased, as is observed to a small degree in Figure 5*b*, and a high-temperature CRM would be produced.

Whatever the explanation, when the laboratory field and the NRM are not close to parallel to each other, systematic changes in the apparent direction of NRM toward the TRM direction can be a sensitive indicator of alteration in the TRM spectrum. In this case the PTRM checks do not indicate marked changes in the TRM spectrum until the specimen is heated to 325°C, and the first point to deviate significantly from the straight line toward higher TRM is at 300°C. The change in apparent direction of NRM, however, is significant for all points beyond 196°C. We have used only the four points from 121° to 196°C and find a very low quality (3.5) paleointensity of 0.096 Oe.

The mean paleointensity for a given flow is computed by using weighting factors that involve the quality factor for each determination (refer to the appendix). The weighted mean paleointensity of the three determinations for this flow is 0.143 Oe, almost identical with the single highest quality paleointensity. If the three determinations had been given equal weight, then the mean would have been about 8% higher. Hence the two very poor values contribute almost nothing to the weighted mean. They do contribute significantly to the

standard error of the mean $\sigma_F = 0.040$ Oe, which weights each value equally (equation (5)). This standard error is more than 4 times the standard deviation $\sigma_F = F_L\sigma_b$ estimated by the least squares procedure for the single high-quality determination. Such is usually the case, and studies of historic Hawaiian lava flows of known paleointensity confirm that sample-to-sample scatter is a better measure of the error associated with the mean paleointensity recorded by a single lava flow.

In summary, we see from Table 2 that of 28 specimens studied by the Thelliers' method, only six were rejected. The three specimens from the Puu Kole flow were rejected because the direction of NRM changed systematically during the intensity experiments throughout the entire range of blocking temperatures. They appear to have acquired a strong secondary component of magnetization, probably isothermal remanent magnetization (IRM) because it is effectively removed by af cleaning at 150 Oe but not by thermal cleaning. The other three were rejected because their NRM-TRM curves were not straight enough ($f < 0.15$), probably owing to alteration of TRM spectra during heating in the laboratory.

In comparing the quality of individual estimates with the magnetic properties revealed in the J_s-T experiments, we see that better results were obtained for the 10 specimens with predominantly single high or low Curie temperatures (average $q = 26.9$) compared to those for the 12 specimens with double or distributed (?) Curie points (average $q = 9.8$). This is in accord with intensity results for Hawaiian historic basalts heated in vacuum [*Khodair and Coe,* 1975].

Overall, the intensity results appear to be fairly good with regard to internal consistency among specimens from the same flow. The average standard error of the paleointensities for the seven flows having three or more individual results is ±0.035 Oe, that is, about ±10%. We believe these estimates of the error to be reasonable ones.

Discussion

We may conveniently compare these values with worldwide intensities (derived mainly from archeomagnetic studies) during the past 8500 years (Figure 6) by recasting them in terms of their equivalent virtual dipole moments (VDM's, *Smith* [1967]). The mean of the eight VDM's in Table 2 is 9.32×10^{25} emu cm^3, with s.d. = 3.69×10^{25}. *Kono* [1971] has summarized published paleointensity results obtained by the Thelliers' method for geologic materials to 10 m.y. old; for 78 determinations he calculated an average VDM of 8.9×10^{25} emu cm^3, with s.d. = 3.4×10^{25}. The intensities that we obtained in this study are therefore all quite normal. The radiocarbon-dated Hawaiian lavas span about twice the time of the archeomagnetic data, but the spread of their VDM's (3.7×10^{25} to 13.0×10^{25} emu cm^3) is very nearly the same. This in itself might be taken as evidence in support of the hypothesis that the nondipole field was low in Hawaii because the averages of worldwide archeomagnetic data given in Figure 6 are thought to represent approximately the changes in moment of the earth's dipole field. Closer inspection of Figure 6 shows that such a conclusion is not warranted and suggests, in fact, just the opposite. It is evident that the VDM's for the Hawaiian lavas dated 2600–4600 years B.P., which are the only ones for which direct comparison is possible, lie consistently above the mean archeomagnetic curve, and we offer three possible inter-

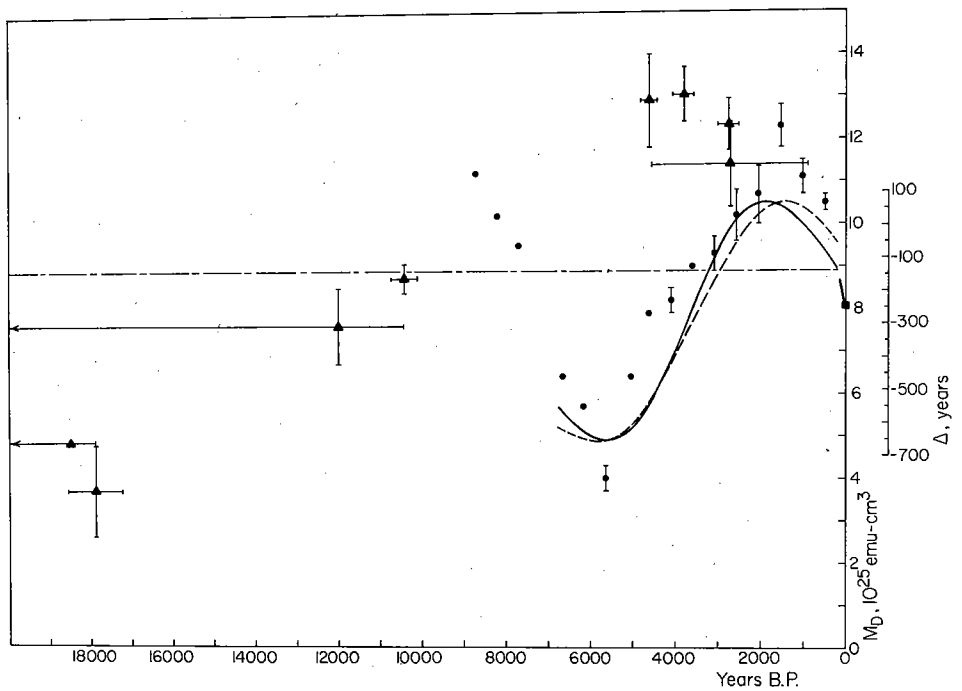

Fig. 6. Virtual dipole moments as a function of age in radiocarbon years before 1950, using the 5730-year half life for ^{14}C. Triangles are data from this study, with uncertainties (Tables 1 and 2). Square is present VDM, the short heavy line segment indicating historic trend from observatory data [*Smith,* 1967]. Circles are mean values from *Cox* [1968] for 500-year class intervals. Solid curve is best fit sinusoid of *Bucha* [1970, 1971] from archeomagnetic data, transformed to radiocarbon years. Dashed curve is VDM variation predicted by differences between radiocarbon years and dendrochronologic years [*Damon et al.,* 1972; *Lingenfelter and Ramaty,* 1970] normalized to maximum and minimum of Bucha's curve. This curve may also be used with the scale on the right to read the difference Δ between radiocarbon age and tree ring age. Short- and long-dashed line is the 10-m.y. average VDM obtained by *Kono* [1971] from published paleointensity results using the Thelliers' method with geologic materials.

pretations: (1) Our estimates of paleointensity are spuriously high. (2) Our paleointensity values are correct and truly represent the dipole field. (3) Our paleointensity values are correct and lie above the archeomagnetic curve because of significant nondipole sources in the vicinity of Hawaii during the time 2600–4600 years B.P.

The first possibility is very unlikely: 11 specimens from 4 flows all yielded high values of ancient field intensity, and 4 of the determinations were of excellent quality ($q > 25$, see Table 2). The second possibility requires further attention. We can discount as unlikely the explanation of the high field values in terms of very short periods of anomalously strong dipole moment. The changes would have to occur extremely fast (within at most a few hundred years), and the likelihood that all four lava flows were extruded during such brief intervals of high fields is very small. The crucial question is, How accurately do the archeomagnetic data describe the time-averaged variation of the actual intensity of the dipole field?

Cox [1968] averaged the VDM's of the past 8500 years in class intervals of 500 years and remarked upon the roughly periodic variation with time. The points that he obtained are replotted in Figure 6; the ones without bars of standard error are those that he considered unreliable because of too few data (three or fewer determinations). *Bucha* [1970, 1971] treated the same problem in a slightly different way, first constructing curves of VDM relative to time for three widely separated regions around the world (Central Europe, Japan, and Mexico and Arizona) and then fitting their average with a sine function expressed in years corrected for the differences between ^{14}C years and dendrochronological years [*Bucha,* 1970]. We have used the conversion tables of *Damon et al.* [1972] to convert Bucha's average curve to ^{14}C years (Figure 6, solid curve). The curve of *Bucha* [1970, 1971] agrees well with the averages of *Cox* [1968] only from 2000 to 2500 years B.P., but the general form of worldwide VDM variation is similar. Bucha and Cox used somewhat different data sets: *Cox* [1968] used data from several other parts of the world, but *Bucha*'s [1971] data were much more complete for the regions that he considered. For the present purpose, Bucha's technique of averaging would appear preferable.

Additional support for the archeomagnetically determined variation of the earth's dipole moment can be inferred from the strikingly similar variation of the rate of ^{14}C production in the atmosphere deduced from the differences between dendrochronologic and radiocarbon dates [*Bucha,* 1970, 1971]. The causal link is the screening of the radiocarbon-producing cosmic ray flux by the geomagnetic field. This screening depends mostly on the dipole moment, the effect of the more localized nondipole features tending to be averaged out. *Lingenfelter and Ramaty* [1970] have shown that for values of the dipole moment between about 2×10^{25} and 20×10^{25} emu cm^3 the production of radiocarbon varies inversely as the square root of the dipole moment. If this relation is used and it is assumed that excess or deficiency of atmospheric radiocarbon is directly proportional to production rate, the variation of dipole moment can be predicted. To do this, we have used excess and deficiency of radiocarbon calculated from the tabulated values of differences between ^{14}C years and tree ring years for the past 6700 ^{14}C years B.P. given by *Damon et al.* [1972]. These differences were obtained by regression analysis of several hundred data points; the resulting function is a nearly perfect sinusoid with respect to the tree ring date [*Damon et al.,* 1972]. We calculated the variation of dipole moment from the variation in radiocarbon concentration and normalized it to the maximum and minimum of Bucha's archeomagnetic curve, as shown in Figure 6 (dashed curve). As it turns out that the predicted dipole moment is very nearly proportional to the difference between ^{14}C age and tree ring age, the scale for Δ in years on the right side of Figure 6 is almost linear. We note, however, that the normalization of the radiocarbon curve to Bucha's archeomagnetic curve has no quantitative physical significance except that the two have nearly identical shapes when this is done.

From Figure 6 one sees that the radiocarbon age discrepancy lags the archeomagnetic data by several hundred years (750 years at present and about 500 years at 1500–2000 years B.P.), as is predicted by theory [*Lingenfelter and Ramaty,* 1970; *Damon,* 1970]. The fact that there appears to be no phase lag at about 5000 years B.P. could easily be due to error in the archeomagnetic dipole moment curve: prior to 3660 years B.P. the archeomagnetic curve is constrained only by the Central European and Japanese data, and prior to 4460 years B.P. only by the Central European data [*Bucha,* 1970, 1971]; the actual period of the dipole moment may be somewhat longer than that shown in Figure 6. Such detailed discrepancies notwithstanding, the general congruence of the radiocarbon and dipole moment curves is impressive, especially when allowance for a phase lag of several hundred years is made.

In summary, we suppose that the curve of *Bucha* [1970, 1971] is a reasonable approximation of the true time-averaged variation for at least the past 4600 radiocarbon years. For a crude estimate of error in the dipole moment at any particular time, we may use the standard error of the mean of the three regional curves used by *Bucha* [1970, 1971]. These curves exhibit large variability between 500 and 2500 years B.P. and are smoother for earlier times, but this may result from greater abundance of data for more recent times. Hence we have applied the percentage uncertainty for the dipole moment at 2570 years B.P. ($\pm 9\%$) to the earlier points at 3890 and 4600 years B.P.

Carrying through with the analysis of error, we find (Table 3) that the visual impression conveyed by Figure 6 is correct: the three paleointensities from well-dated Hawaiian flows between 2600 and 4600 years B.P. are each significantly higher than the estimated dipole field for the same time period, and the average difference is very highly significant, about 8 times the standard error (0.211 ± 0.028 Oe at Hawaii, or $(5.00 \pm 0.65) \times 10^{25}$ emu cm^3 in terms of moment). From this we conclude that the nondipole field in the Hawaiian region must have been rather strong during this time to produce these differences in intensity from the dipole field.

Estimating the complete vector for the nondipole field at the time of extrusion of these three lava flows facilitates comparison with the modern nondipole field. If we assume a position for the geomagnetic pole in the past, then we can use the archeomagnetically determined values of dipole moment to calculate the components of the ancient dipole field. We use the present position of the geomagnetic pole because many of the archeomagnetic determinations of moment include this assumption and also because the average VGP for our radiocarbon-dated lavas lies very close to it (Figure 1; also see the discussion below on dispersion of directions).

The differences between our paleomagnetically determined field components and those of the ancient dipole field yield estimates for the northward, eastward, and downward components of the ancient nondipole field at Hawaii (Table 3). Compared with the present, these correspond to a strong nondipole field in Hawaii during that time, on the average

TABLE 3. Scalar and Vector Differences Between Predicted and Observed Ancient Field at Hawaii

Flow Name and Age	F_D, Oe	$\bar{F}_E - F_D$, Oe	ΔF North, Oe	ΔF East, Oe	ΔF Down, Oe	$\lvert\Delta F_{ND}\rvert$, Oe	M_D, $\times 10^{25}$ emu cm^3	VDM $- M_D$, $\times 10^{25}$ emu cm^3
Visitor Center, 2570 years B.P.	0.448 ± 0.040	0.132 ± 0.049	0.079	−0.050	0.122	0.154	10.05 ± 0.91	2.29 ± 1.10
Waiohinu, 3790 years B.P.	0.334 ± 0.030	0.214 ± 0.040	0.187	0.117	0.059	0.228	7.52 ± 0.68	5.52 ± 0.93
Hale Pohaku, 4600 years B.P.	0.257 ± 0.023	0.286 ± 0.053	0.246	0.131	0.099	0.296	5.74 ± 0.52	7.18 ± 1.11
Average difference (absolute)		0.211 ± 0.028	0.171	0.099	0.093	0.226	7.77 ± 1.08	5.00 ± 0.65

F_D is total field predicted at Hawaii, calculated from dipole moment (M_D) values of *Bucha* [1971] by assuming dipole orientation as at present (78.6°N, 290.6°E). $\bar{F}_E - F_D$ is scalar difference, using $\bar{F}_E$ values from Table 2. ΔF is vector components of differences between predicted and observed fields, using components of F_D and directions and intensities in Tables 1 and 3. $\lvert\Delta F_{ND}\rvert$ is magnitude of vector difference between predicted and observed fields. M_D is dipole moment values of *Bucha* [1971]. VDM $- M_D$ is scalar difference using data in Table 2. Maximum of each component of 1945 nondipole field for ΔF north, ΔF east, and ΔF down is −0.130, −0.132, and −0.173 Oe, respectively [*Bullard et al.*, 1950]. Maximum intensity of 1965 international geomagnetic reference field for $\lvert\Delta F_{ND}\rvert$ is ~0.19 Oe [*Doell and Cox*, 1972].

slightly stronger than the most intense regions of both the 1945 and the 1965 nondipole fields (see Table 3). Errors in the estimates of paleointensity, in the ^{14}C dates for the lava flows, in the archeomagnetic estimates of dipole moment, and in the choice of the position of the ancient geomagnetic pole would affect the individual values of ancient nondipole field components but not the general conclusion.

Assuming that these large nondipole field intensities each arose from a single simple geomagnetic feature similar to modern nondipole foci, we can try to estimate the approximate position and intensity of these features. To do so, we represent the feature by a radial dipole displaced from the center of the earth by 0.28 of the earth's radius. *Alldredge and Hurwitz* [1964] have shown that the 1945 field [*Vestine et al.*, 1947*a*] can be modeled quite well by one central dipole and eight such eccentric dipoles, and *Cox* [1968] has pointed out that the unreasonably great depth of the eccentric dipoles below the core-mantle boundary is an artifact of using a point dipole to model an extended source which probably lies not far below the core-mantle boundary.

Each nondipole field vector in Table 3 could be produced by one of two eccentric dipoles at different latitude and longitude, one with an inward pointing (negative) moment and the other with an outward pointing (positive) moment (see Figure 1*a* of *Coe* [1977] for an illustration of this). The dipole nearer the site on the earth where the nondipole field is known has a weaker moment than the dipole which is farther away. Without field determinations for the same time from at least two significantly separated places, there is no way to select rigorously between the two solutions. Usually, we favor the nearer dipole as being a more likely approximation of the true source. When both solutions are about the same angular distance θ from the site, which occurs where $\theta \approx 65°$ and corresponds to the situation where the nondipole field is nearly horizontal, neither solution is more reasonable than the other. Indeed, inspection of the map of the 1945 nondipole field [*Bullard et al.*, 1950] suggests that a single source would rarely dominate the nondipole field to distances greater than 50°–60° from its center, and for such cases it is unlikely that the assumption used for these calculations of a single nondipole source will remain valid.

In Table 4 we give the nearer and farther solutions for eccentric dipoles under the assumption that the dipole field was either inclined the same as at present or was axial. The plus and minus values bracket the extreme range of variation of latitude, longitude, moment, and angular distance to the site from the eccentric dipole when the uncertainties in both the paleointensity ($\bar{F}_E$ in Table 2) and the intensity of the ancient dipole field (F_D in Table 3) are taken into account. For the data from the 2570-year-B.P. flow the nearer solution for the eccentric dipole is only about 30° from the site, whereas the farther solution is about 100° away. In this case we favor the nearer solution, which has a negative moment about $\frac{1}{4}$ the strength of the total dipole moment of the present field of the earth. This is typical of the strength of the eccentric dipole moment found by *Alldredge and Hurwitz* [1964] for the modern field.

For the data from the two flows at 3790 and 4600 years B.P.,

TABLE 4. Hypothetical Radial Eccentric Dipoles

Main Dipole Orientation	Nearer Solution: Latitude, °N	Longitude, °E	M, $\times 10^{25}$ emu cm^3	θ, deg	Farther Solution: Latitude, °N	Longitude, °E	M, $\times 10^{25}$ emu cm^3	θ, deg
Visitor Center, 2570 Years B.P.								
Inclined*	46^{+7}_{-17}	180^{+8}_{-12}	$-1.2^{+0.6}_{-0.4}$	33^{+2}_{-1}	-56^{+32}_{-11}	275^{+37}_{-29}	$4.1^{+1.6}_{-1.4}$	96^{+1}_{-2}
Axial	45^{+6}_{-17}	218^{+3}_{-2}	$-1.0^{+0.5}_{-0.6}$	27^{+5}_{-10}	-69^{+21}_{-3}	133^{+29}_{-37}	$3.9^{+1.7}_{-1.6}$	102^{+5}_{-6}
Waiohinu, 3790 Years B.P.								
Inclined	59^{+2}_{-3}	264^{+7}_{-5}	$-3.7^{+0.6}_{-0.6}$	58^{+3}_{-2}	-42^{+5}_{-3}	161^{+1}_{-1}	$5.2^{+1.4}_{-1.4}$	73^{+2}_{-3}
Axial	49^{+4}_{-5}	268^{+4}_{-4}	$-4.2^{+0.4}_{-0.5}$	58^{+3}_{-2}	-34^{+7}_{-5}	152^{+2}_{-2}	$5.8^{+1.3}_{-1.2}$	73^{+2}_{-3}
Hale Pohaku, 4600 Years B.P.								
Inclined	61^{+1}_{-2}	258^{+5}_{-6}	$-4.4^{+0.9}_{-0.9}$	56^{+2}_{-1}	-46^{+3}_{-2}	164^{+1}_{-1}	$6.9^{+1.8}_{-1.8}$	75^{+1}_{-2}
Axial	55^{+2}_{-4}	263^{+5}_{-4}	$-4.7^{+0.8}_{-0.8}$	56^{+2}_{-1}	-40^{+5}_{-3}	156^{+2}_{-3}	$7.3^{+1.7}_{-1.7}$	75^{+1}_{-2}

Latitude north and longitude east are coordinates of radial eccentric dipole. M is moment of radial eccentric dipole (negative values mean that dipole is directed inward); θ is great circle distance between coordinates of radial dipole and sampling site.
*Present geomagnetic dipole (78.6°N, 290.6°E).

TABLE 5. Mean Paleomagnetic Poles and Angular Dispersions of VGP's, Brunhes Epoch, Hawaiian Islands

Island and Lava Series	Reference	N	PLA, deg	PLO, deg	α_{95}, deg	S, deg	S_L, deg	S_u, deg
Hawaii								
Historic	Table 6, this paper	17	80.4	292.4	1.4	3.3	2.6	4.3
^{14}C dated	Table 1, this paper	8	78.4	301.1	10.7	15.5	11.4	24.4
Kau	*Doell and Cox* [1965]	54	81.5	61.3	0.8	3.3	2.9	3.8
Puna	*Doell* [1969] and unpublished data of R. R. Doell and E. A. Mankinen (1972) for 26 additional lavas	44	86.9	226.9	1.4	5.1	4.5	6.0
Kahuku	*Doell and Cox* [1965]	29	79.7	336.4	4.4	13.3	11.2	16.3
Hamakua	*Doell and Cox* [1965]	11	72.5	243.2	2.4	4.2	3.2	6.1
Ninole	*Doell and Cox* [1965]	25	84.6	21.6	3.9	11.5	9.6	14.3
Pololu	*Doell and Cox* [1965]	29	82.6	314.1	2.9	8.6	7.3	10.6
Niihau, Kiekie	*Doell* [1972*c*]	11	79.8	63.3	4.9	8.7	6.7	12.6
Oahu, Honolulu	*Doell* [1972*b*]	25	86.4	20.9	3.4	9.4	7.8	11.7
Selected Brunhes epoch*		129	84.8	331.5	1.9	12.7	11.7	13.9

N is number of lava flows. PLA and PLO are north latitude and east longitude of mean of VGP's. S is measured total angular standard deviation of VGP's calculated with respect to each mean pole. S_L and S_u are lower and upper 95% confidence limits of S, respectively [*Cox*, 1969].

*Includes only ^{14}C-dated, Kahuku, Hamakua, Ninole, Pololu, Kiekie, and Honolulu series and omits lavas with $\alpha_{95} > 7°$.

however, the nearer solution yields eccentric dipoles that are 58° and 56° away from the sites, respectively, only 15° and 19° closer than the solutions for the more distant dipoles. At these times it is probable that two or more sources were contributing significantly to the nondipole field in Hawaii, and, as was stated above, there are an infinite number of possible solutions with different configurations and strengths of moment. One efficient solution that is reasonable in terms of the modern nondipole field consists of two eccentric dipoles with inward and outward directed moments, respectively, at approximately the same positions as the nearer and farther solutions listed in Table 4. Even this very efficient configuration would require moments at least 40% stronger than the strongest eccentric dipoles computed by *Alldredge and Hurwitz* [1964] for the modern field.

It is of interest to compare our paleomagnetic results for the nondipole field with the hypothesis put forward recently by *Cox* [1975]. He postulates that the drifting part of the nondipole field is biased in such a way that sources of outward directed flux lie most frequently at low latitudes, roughly between 35°N and 35°S, and that sources of inward directed flux lie generally at higher latitudes. This is the case with the present nondipole field. Such a distribution of drifting nondipole sources can explain the anomalies of average inclination (more negative than that due to an axial geocentric dipole) first identified by *Wilson* [1970, 1971, 1972] in the paleomagnetic data from Quaternary and Tertiary time.

The source derived for the 2570-year-B.P. nondipole field (Table 4) is inward directed at a latitude of about 45°N, in agreement with the predicted distribution of *Cox* [1975]. The sources calculated for the 3790- and 4600-year-B.P. nondipole fields are more ambiguous. The 'efficient' configuration for either of them, as discussed above, with an outward directed source between 35° and 45°S and an inward directed source between 50° and 60°N, roughly fits the predicted distribution. Other aspects of the paleomagnetic data are less suggestive of a drifting but latitudinally biased nondipole field. As was pointed out earlier, the average VGP for all the flows lies to the right side, not the far side, of the north pole as viewed from Hawaii (Figure 1). In other words, a negative inclination anomaly is not observed but rather an eastward declination anomaly. This is even more striking if we restrict our attention to the six flows of age less than 10,400 years. Moreover, the nondipole fields, and hence most likely the configuration of the sources, for 3890 and 4600 years B.P. are very similar, not an expected result if westward drift of the nondipole field had been occurring at anywhere near the present rate. These facts are most simply interpreted as arising from more localized sources whose intensity grows and decays, something like the standing field of *Yukutake and Tachinaka* [1969], though not truly stationary. A similar hypothesis has recently been advanced by *Creer* [1977] to explain paleomagnetic secular variation.

DISPERSION OF PALEOMAGNETIC DIRECTIONS

The dispersion of VGP's illustrated in Figure 1 for the radiocarbon-dated lavas is unexpectedly large. The total measured angular standard deviation of these VGP's is 15.5° (Table 5), as compared to 10.8° for 219 Brunhes age lava flows on Hawaii found by *Doell and Cox* [1972]. The 95% confidence intervals only barely overlap, an indication that the difference in these populations is fairly significant. In Table 5 we summarize the mean VGP positions and angular dispersions of VGP's for all the Brunhes epoch lava series in the Hawaiian Islands from which extensive collections were made. The angular dispersion of 10.8° cited by *Doell and Cox* [1972] was obtained from approximately this same data set, with the following differences: 12 of the 17 historic lavas (Table 6) were included, and neither the ^{14}C-dated lavas nor the Kiekie series was included (R. R. Doell, written communication, 1972).

One might wonder whether the high dispersion of the ^{14}C-dated lavas could be caused by sources other than secular variation. The various sources of dispersion of NRM have been thoroughly analyzed by *Doell and Cox* [1963]. For the present purpose we lump these sources into three categories: S_w, due to within-flow variation of individual measurements; S_s, which arises in cases where the sampling sites are scattered over the volcanic edifice and, because of the magnetization of underlying lavas, the local field is not everywhere parallel to the regional field; and S_{sv}, due to secular variation. For the groups of lava flows listed in Table 5, S_s contributes to the observed dispersion of VGP's only for the historic, ^{14}C-dated, Kiekie series, and Honolulu series lavas, all collected from sites widely distributed on their respective volcanic edifices.

For the island of Hawaii we can use the relation $S_s^2 = S^2 - S_{sv}^2 - S_w^2/N$ to estimate S_s from the data for the historic lavas by assuming that the observed dispersion contains only a negligible contribution from secular variation, that is, $S_{sv} = 0$. (Here N is the average number of specimens per lava flow.) This assumption is supported by the low value of S_{sv} at Hawaii since 1900 [*Doell and Cox,* 1963] and by the fact that the NRM directions in the historic lavas show no serial correlation. The mean within-flow dispersion of NRM directions in the historic lavas is 4.5°, which corresponds to $S_w = 4.0°$ for VGP's assuming Fisherian distributions of within-flow NRM directions and using equation (12) of *Cox* [1970]. Hence if $S_{sv} = 0$, the maximum estimate of S_s for the historic lavas is 2.9°. For the ^{14}C-dated lavas, S_w is 5.1°, computed from the Cox equation, and because the site distribution over the island is as broad as that for the historic lavas, we use the same value of S_s. Then from $S_{sv}^2 = 15.5^2 - 2.9^2 - 5.1^2/6.75$, the value of S_{sv} for the ^{14}C-dated lavas is 15.1°; that is, correcting the observed value of S for site distribution and within-flow dispersion reduces it by only 0.4°. Hence it appears that a higher amplitude of secular variation has been recorded by the ^{14}C-dated lavas than has been recorded by any of the other sampled lava series on Hawaii. (In Table 5 we give the total measured angular dispersions of VGP's only, without attempting to make corrections for S_s and S_w.)

Of the ten series of lava flows listed in Table 5, four have very low angular dispersions of VGP's (historic, Kau, Puna, and Hamakua). Two of these (Kau and Puna) consist together of 98 lava flows, almost half the number averaged for the total dispersion figure of 10.8° cited by *Doell and Cox* [1972]. The Kau and Puna series differ from all other in Table 5 in that they were sampled in sections very close to their respective eruptive centers: the Kau series was sampled in a 140-m section comprising the full height of the northwest wall of Mokuaweoweo, the summit caldera of Mauna Loa [*Doell,* 1969]; 35 Puna series lavas were sampled on Uwekahuna Bluff, the west wall of the large summit crater of Kilauea, while the remaining 9 were sampled near the summit of Kilauea, 19 km southeast of Uwekahuna Bluff (R. R. Doell, written communication, 1972). All samples from the other older lava series listed in Table 5 were collected far out on the flanks of their respective source volcanos, most near the present shorelines [*Doell and Cox,* 1965] or from nearly widely separated individual vents [*Doell,* 1972*b, c*]. From this distribution the possibility is apparent that the Kau and Puna series were erupted at much greater rates than the other eight volcanic series, perhaps entirely within only a few hundred years. This would provide an easy explanation for the similarity in paleomagnetic dispersion of the Kau and Puna series and the historic lavas. *Doell* [1969] argued against this for the Kau lavas, using as his main evidence the historic rate of eruption of Mauna Loa. *Doell and Cox* [1972] extended this argument by pointing out that paleointensity variation of a factor of 2 in the Kau series suggested eruption over a period of time of about 10^4 years and cited similar evidence for the Puna series; we will return to this point later. It is fair to say here that the age and time span of both the Kau and the Puna series are not exactly known except that the top flow of the Puna series is very nearly the same age as the Visitor Center flow ($\lesssim$ 2570 years, Table 1) [*Powers,* 1948, 1955].

On the supposition that the data from the Kau and Puna series unduly bias the 10.8° estimate of VGP dispersion, we have calculated the angular dispersion of VGP's for all the lava series in Table 5 except the historic lavas and the Kau and Puna series, excluding the few individual lavas with $\alpha_{95} > 7°$. No lavas were omitted because of low VGP latitudes [*Doell and Cox,* 1972], since none occur in the entire Brunhes data. The result (Table 5) is 12.7°, calculated with respect to the mean of all VGP's; this value matches very well the other data points for the vicinity of latitude 20° shown in the worldwide summaries for the Brunhes epoch and for the past 5 m.y. illustrated by *McElhinny and Merrill* [1975]. In other words, if the Kau and Puna series and the historic lavas are omitted from the total Brunhes data set on the supposition that they are unrepresentatively dense samplings of rather short periods of time, there is not very strong evidence that especially low secular variation has been recorded in the Brunhes epoch lavas of the Hawaiian Islands.

A similar conclusion was reached by *Duncan* [1975], who noted that the Kau and Puna series were apparently of recent

TABLE 6. Paleomagnetic Directional Data, Historic Hawaiian Lavas

Year	*SLA*, deg	*SLO*, deg	*N*	$\bar{H}$, Oe	*k*	α_{95}, deg	*I*, deg	*D*, deg	*PLA*, deg	*PLO*, deg
1750*	19.37	205.04	7	100	175	4.6	39.7	5.4	84.1	261.8
1790*	19.48	205.10	9	100	772	1.9	38.8	10.9	79.6	279.7
1800–1801*	19.78	204.08	7	100	501	2.7	34.8	12.2	78.5	295.2
1840*	19.56	205.12	11	100	116	4.3	36.4	6.2	84.1	287.3
1843*	19.69	204.51	7	100	169	4.7	35.1	10.6	80.1	294.7
1852	19.60	204.62	8	0	263	3.4	35.1	8.3	82.2	295.0
1859	19.83	204.18	7	50	461	2.8	36.4	10.7	79.9	290.2
1868*	19.06	204.32	6	100	232	4.4	33.8	9.1	81.4	296.6
1881	19.59	204.56	8	0	464	2.6	33.9	7.5	82.9	301.8
1907*	19.07	204.25	6	100	716	2.5	36.2	10.6	80.0	285.7
1919	19.23	204.12	8	0	469	2.6	29.1	5.6	83.3	326.7
1926	19.20	204.13	8	0	388	2.8	33.8	9.9	80.6	296.8
1935*	19.69	204.51	5	100	479	3.5	37.5	15.3	75.6	286.7
1940	19.50	204.41	8	0	496	2.5	37.3	15.1	75.8	286.4
1950	19.34	204.13	8	0	190	4.0	33.8	9.1	81.4	298.2
1955*	19.44	205.09	10	100	344	2.6	33.8	11.8	78.8	298.0
1960	19.48	205.16	8	0	342	3.0	34.5	14.7	76.1	294.8

SLA and *SLO* are north latitude and east longitude of sampling site. *N* is number of specimens. $\bar{H}$ is peak alternating demagnetizing field, and *k* and α_{95} are precision parameter and radius of 95% confidence cone [*Fisher,* 1953]. *I* and *D* are inclination downward and declination eastward. *PLA* and *PLO* are north latitude and east longitude of VGP.

*Data from *Doell and Cox* [1963].

age, significantly younger than the other volcanic series for which data were published by *Doell and Cox* [1965]. Duncan calculated an angular dispersion of 13.4° with respect to the geographic pole for these older rocks and concluded that the low value of secular variation for Hawaii was restricted to Holocene time. This conclusion apparently should be modified, however, because the ages of the Puna series and probably also the Kau series are contained within the time span of the ^{14}C-dated lavas, which record much higher dispersion.

Finally, *McElhinny and Merrill* [1975], in discussing the relative contributions of dipole wobble and secular variation of the nondipole field to the observed angular dispersions of VGP's, pointed out that the dispersion seen in the Kau series (3.1°) is much less than the 10.8° estimated by *Doell and Cox* [1971, 1972] for the angular dispersion due to dipole wobble alone and that the mean of the Kau series VGP's is displaced 8.5° from the geographic pole. They conclude that if it took 10^4 years for the Kau series to be erupted, then 10^4 years is too short a time to sample the full range of secular variations arising from both dipole and nondipole fields. (This point had already been noted by *Doell and Cox* [1972].) The data from the Puna series (Table 5) could also be taken to support McElhinny and Merrill's conclusion, but perhaps stronger evidence comes from the ^{14}C-dated lavas: the angular dispersion is large and the time span is more than 1.5×10^4 years, yet the mean VGP differs very little from the present dipole or the mean VGP for the historic lavas and is significantly different from the geographic pole (Figure 1 and Table 5). Our data are too few to be conclusive, but studies by *Ozima and Aoki* [1972] and *Aziz-ur-Rahman and McDougall* [1973] also indicate that 10^4 years is too short a time for dipole wobble to be sufficient to produce the 9° dispersion of VGP's that *McElhinny and Merrill* [1975] estimate to originate from this source alone when a much longer time is considered.

Comparison With Previous Paleointensity Results

Many paleointensity determinations have been made on lavas of the Kau and Puna series of Hawaii (R. R. Doell, P. J. Smith, and E. A. Mankinen, unpublished data, 1968–1969), and a preliminary account of these was published by *Doell and Cox* [1972]. The determinations were made by the method of *Wilson* [1961], in part as modified by *Doell and Smith* [1969]. Almost twice as many individual determinations were made as were published in the summary diagram shown by *Doell and Cox* [1972], but addition of the newer and more complete data does not alter the aspect of those diagrams significantly. Doell and Cox noted that the paleointensity variation recorded in the Kau and Puna series was large, and they used this fact and the historic eruption rates of Mauna Loa and Kilauea volcanos to argue that the Kau and Puna series were each erupted over a period of several thousand years rather than several hundred. Because we suspect, as we discussed above, that both lava series may have been erupted very rapidly, we have reexamined the original paleointensity data in detail.

Four factors can be cited in favor of these earlier results: (1) Both lava series seem to show stratigraphically progressive changes in apparent paleointensity. (2) The within-flow variation in both lava series is no greater on the whole than our results using the Thelliers' method. (3) More than 5 times as many lavas were investigated in the Kau and Puna series than were investigated in the ^{14}C-dated lavas. (4) In the Puna series the apparent paleointensity variations do not seem to correlate with any other magnetic property.

The following five factors, however, cause us to be dubious about the Puna and Kau paleointensities. (1) They were determined by using a method that is demonstrably inferior to the Thelliers' method [*Coe and Grommé*, 1973] because no intensity ratios are obtained before the specimens are heated to 600°C to impart the artificial TRM. (2) The experiments were done in air and *Khodair and Coe* [1975] have shown that much more nearly correct paleointensities are obtained from basalts when they are heated in vacuum. (3) The thermomagnetic curves (J_s-T) for the Puna series specimens are irreversible in air. In most cases the magnetizations after cooling from 600°C were about 10% less than the original values, and the heating and cooling curves differed significantly in shape. (4) In the Kau lavas, although the J_s-T curves were reproducible in air, heating the specimens more slowly to 600° in air to produce TRM caused significant changes in blocking temperature distributions. Relative to the blocking temperatures of NRM, about half the TRM blocking temperature distributions are shifted to higher temperatures, and about half to lower temperatures. The directions and amounts of these changes are fairly well correlated with the apparent paleointensities themselves, so the twofold variation in apparent paleointensity in the Kau lavas [*Doell and Cox*, 1972] may be an artifact arising from petrological differences. (5) Our intensity determination for the Visitor Center flow does not match any of those from the top of the Puna series, although they are probably the same age. The top flow in the Uwekahuna Bluff section of the Puna series (elevation, 1225 m) and the Visitor Center flow (elevation, 1201 m where it was sampled by us and 1213 m where it was dated at Volcano House [*Powers*, 1948, 1955, and personal communication, 1966]) are part of the top surface of Kilauea volcano that existed prior to the caldera subsidence that formed Kilauea crater some time in the past 2600 years. The paleointensity determinations by Wilson's method from the nine flows spanning the uppermost 70 m of Uwekahuna Bluff average 0.47 Oe with little variation (s.d. = 0.03 Oe), whereas our own determination from the Visitor Center flow is 0.580 ± 0.029 Oe.

If the variations in apparent paleointensity in the Puna and Kau series are real, the fact that they are not accompanied by appreciable changes in paleofield direction would lead to two possible interpretations. The first, favored by *Doell and Cox* [1972], is that these lavas actually do record changes in the dipole field during times of unusually low secular variation of the nondipole field. If this is so, the parts of the Puna and Kau series from which the paleomagnetic data were obtained were probably erupted over periods of several thousand years, but these periods cannot have overlapped because their respective mean VGP's are very different (Figure 1). This is at variance with the fact that while all of the Puna series and probably much of the Kau series were erupted within the time spanned by the ^{14}C-dated lavas, the ^{14}C-dated lavas show large variations in intensity and direction. As defined by *Stearns and McDonald* [1946], the Puna series and the Kau series form and cover the carapaces of Kilauea and Mauna Loa volcanos, respectively, and stratigraphically overlie a widespread ash known as the Pahala ash. This ash is associated with the ^{14}C-dated lavas at Maniania Pali and Hilina Pali, but because the ages there are 10,410 and 17,860 years B.P., respectively, there is some question about whether the ash layers represent a single eruptive episode. The maximum age of the part of the Kau series exposed in Mokuaweoweo was estimated by *Doell* [1969] to be about 10,000 years on the basis of the absence of the Pahala ash from the summit of Mauna Loa and from

within the Kau series lavas at that place. It is possible, however, that the Pahala ash was never deposited high on Mauna Loa or at least not in sufficient amount to be visible at this time; if this is so, the part of the Kau series exposed in Mokuaweoweo caldera could be somewhat older than any of the ^{14}C-dated lavas.

The second possible interpretation is that the data from the Puna and Kau series represent two different times during which secular variation of the nondipole field was large but was manifested at Hawaii almost entirely by changes in field intensity alone. This might seem to require near coincidence of the nondipole and dipole field directions. *Stacey* [1969, p. 139] has suggested this as a general explanation for the low angular dispersion of paleomagnetic directions at Hawaii and refers briefly to measurements between 1902 and 1938 at the Honolulu geomagnetic observatory as supporting this hypothesis. We have examined the Honolulu observatory data for the interval 1905–1945 as diagramed by *Vestine et al.* [1947*b*] and have come to the opposite conclusion. The disagreement arises because Stacey did not separate the relative contributions to the total secular variation of the secular variations of the dipole and nondipole fields, which, during that time at Honolulu, were about equal in total magnitude. We have performed the separation for the 1905 and 1945 fields at Honolulu using the epoch 1945 harmonic coefficients and their secular variations back to epoch 1905 as given by *Vestine et al.* [1947*a, b*] and the dipole harmonic coefficients calculated by *McDonald and Gunst* [1967] from the data of Vestine et al. For this time interval the average magnitude of the nondipole field is 0.016 Oe, and it is directed at an angle of 90° to the total field. More important, the vector change of the nondipole field during the 40-year interval is 0.0118 Oe, and this vector makes an angle of 57.4° to the total field for epoch 1905. For comparison, the vector change in the dipole field during the 40-year period is 0.0098 Oe at an agle of 171° to the 1905 dipole field. In other words, the main change in the dipole field is a decrease in its intensity [*McDonald and Gunst,* 1967], but the change in the nondipole field is not nearly parallel either to itself or to the total field.

The angular dispersion expected if a set of vectors, all of magnitude 0.0118 Oe but having random orientations, were added to the 1905 total field (magnitude 0.3779 Oe) is 1.45° [*Cox,* 1970]. The observed angular change in the total field at Honolulu for the 40-year interval is 1.25°, and if the contribution due to the dipole field change is subtracted, the angular change becomes 1.53°. Hence the actual change in field direction at Honolulu is commensurate with that expected if it were due to a randomly fluctuating nondipole field.

It could still be argued, of course, that *Stacey*'s [1969] explanation is the correct interpretation of the low paleomagnetic dispersion at Hawaii, even though it has not been true since 1905. In fact, a case might be made that our own data support this explanation. The three nondipole vectors that we have explicitly determined (Table 3) are more nearly parallel to the dipole field than they would be if they were randomly directed; the angles of departure range from 19° to 38°. The observed angular standard deviation for all eight lava flows is at least 50% lower than the most probable value that would be calculated by using the statistical methods of *Cox* [1970] if the dispersion of the eight directions were due to randomly oriented nondipole components as large as we find for the interval 2600–4600 years B.P. (Table 3). Alternatively, our nondipole field estimates may be too high (especially for Hale Pohaku) owing to a combination of the sources of error discussed earlier. For the Puna and Kau series, however, the degree of parallelism of nondipole and dipole fields would have to be improbably close to account for their extremely low paleomagnetic angular dispersions if large nondipole field changes are taken as the explanation of their apparent paleointensity variations.

If we weigh the arguments given in this section, it seems to us more likely that the parts of the Puna and Kau series exposed in their respective caldera walls were accumulated during short time intervals and therefore show little variation in paleomagnetic direction. The large apparent paleointensity variations in these two lava series probably arise to a significant extent from petrologic factors and the limitations of the method used.

STATUS OF THE PACIFIC NONDIPOLE LOW

Various studies of the past few years have made the hypothesis of a long-standing low of the nondipole field in the central Pacific less tenable. In addition to the reevaluations of the Hawaiian directional data described earlier, the possible extent of the area of the low has been increasingly limited by the discovery of angular dispersion not significantly lower than would be predicted by the standard secular variation model based on the present field [*Cox,* 1970]. Such values of angular dispersion of VGP's have been found in the Galápagos Islands [*Doell and Cox,* 1972] and Easter Island [*Isaacson and Heinrichs,* 1976] for the past 0.7 m.y. and in the Society Islands [*Duncan,* 1975] for the past 3.4 m.y. Angular dispersion of VGP's determined in the Aleutian Islands [*Bingham and Stone*, 1972] is significantly lower than the standard model for 57 lavas less than 1 m.y. old but fits the standard model well for the entire set of 90 lavas of late Tertiary and Quaternary age. This apparent tendency for angular dispersion of NRM to be lower in younger lava sequences has been noted for many parts of the world by *Doell and Dalrymple* [1973] (see also *Duncan* [1975]), and it clearly raises questions concerning the periods of secular variation and the problems of obtaining representative sampling [*McElhinny and Merrill,* 1975].

In the Hawaiian Islands themselves, near the center of the present low in the nondipole field, *Cox* [1975] has reinterpreted the paleomagnetic data [*Doell and Cox,* 1965; *Doell,* 1972*a, b, c*; *Doell and Dalrymple,* 1973] in terms of quiet and noisy times of the geomagnetic field. The noisy times are considered to occur when large features of the nonstationary part of the nondipole field drift westward in the vicinity of Hawaii. This model of *Cox* [1975] does not address the question of whether the nondipole field, averaged over quiet and noisy times, was abnormally low in the region of Hawaii.

Duncan [1975] and *McElhinny and Merrill* [1975] have concluded that the low nondipole field in Hawaii is a recent phenomenon, probably restricted to Holocene time, on the basis that the large proportion of data from the Puna and Kau series excessively biases the observed angular dispersion toward a low value. The large angular dispersion that we have found in the ^{14}C-dated lavas suggests that the Puna and Kau series, where they were sampled in caldera walls, record very low angular dispersion not because they are Holocene but rather because they were erupted so rapidly that they did not record nearly as large an amplitude of secular variation as did most of the other Hawaiian lava series. Our paleointensity results strongly support this interpretation; they show that even the very limited conclusion of a low nondipole field in the vicinity of Hawaii during Holonene time is unlikely. We have inferred the existence of a significant nondipole field in Hawaii

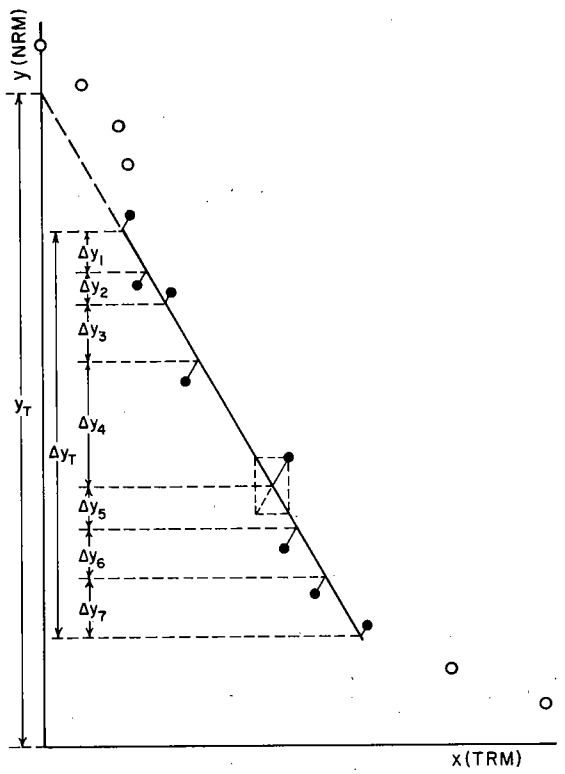

Fig. 7. Hypothetical NRM-TRM diagram illustrating statistical parameters. Open circles are rejected points; solid circles are points used to calculate slope of least squares line (solid line). Small rectangle shows geometry of adjustment of individual points to least squares line [*York*, 1967]. Total extrapolated NRM is y_T, fraction of NRM used for paleointensity determinations is Δy, and NRM intervals used in calculation of gap factor Δy_j are j = 1–7.

at 2570, 3790, and 4600 years B.P., and the scatter of virtual pole positions and dipole moments derived from the older ^{14}C-dated lavas also indicate that this has generally been true.

APPENDIX

Analysis of NRM-TRM Curves

There are many factors that may distort the NRM-TRM curves from the ideal straight line [*Coe*, 1967*b*]. We are usually faced with the problem of trying to decide whether there is a segment of the NRM-TRM curve that has been minimally distorted and whose slope still reflects the true paleointensity. It is here that subjectivity may influence the results to an undesirable degree. We have developed a number of criteria in an attempt to keep the subjective element within reasonable bounds.

1. We consider only segments that are defined by at least four points and that span at least 15% of the total extrapolated NRM (Figure 7). We eliminate no anomalous points within the temperature interval of the segment unless we can prove that a mistake was made in the experiments, since an anomalous point commonly signifies real nonideal behavior.

2. We avoid segments that show excessive systematic curvature. By this we mean that no subsegment that spans at least half the length of the chosen segment has a slope that deviates by more than 20% from the overall slope. This criterion is quite arbitrary, but it is easy to apply and assures one of handling the data uniformly once a suitable cutoff percentage has been selected. The rather high cutoff of 20% that we used is necessary because random scatter can produce large deviations in slope of the subsegments when the number of points is small. If we chose a cutoff of 15%, two useful determinations reported in Table 2 would fail, and at 10%, nine would fail.

3. We avoid segments that are contaminated by secondary components of NRM, since these tend to affect low-temperature data most strongly. VRM produces too steep a slope if the paleointensity is much lower than the mean posteruption field and too shallow a slope if it is much higher [*Coe*, 1967*b*]. IRM can readily be detected by changes in direction of NRM during the stepwise thermal demagnetization of the Thelliers' method, unless by chance it is parallel to the original NRM. Flows with significant scatter of directions from specimen to specimen are always suspect, especially if the scatter decreases with af demagnetization.

4. If no secondary components of NRM are suspected, we prefer a low-temperature segment to any high-temperature segments of comparable quality. This preference is borne out by studies of historic Hawaiian basalts that cooled in a known field [*Coe and Groomé*, 1973; *Khodair and Coe*, 1975; A. Khodair, written communication, 1976]. Irreversible changes in the spectra of NRM and TRM are increasingly common and severe as the temperature to which the specimen is heated in the laboratory increases. We commonly guide our choice of maximum cutoff temperature for the segment by redetermining the PTRM at certain lower temperatures after the heating steps have progressed to higher temperatures [*Coe*, 1967*a*, *b*]. Our procedure in these PTRM checks is occasionally to follow a field-off step by one or more field-on steps at lower temperatures. For plotting, the NRM values corresponding to these PTRM check points are obtained by linear interpolation between the bracketing paired heating steps. These PTRM values can thereby be compared with those that had already been determined from the same (or similar) temperatures during the normal sequence of paired heatings. When significant discrepancies in PTRM occur, we can be sure that the TRM spectrum has been altered and that any further data obtained by heating to even higher temperatures will be highly suspect. It is important to remember, however, that the absence of such discrepancies does not prove that the TRM spectrum is unchanged, for alterations of remanence with high blocking temperatures may occur during the normal sequence of steps at lower temperatures. This could arise from chemical changes in the magnetic minerals before their blocking temperatures are attained.

Having identified by the above criteria the series of points associated with the desired segment of the NRM-TRM curve, we now wish to estimate its slope. The usual least squares technique assumes that errors are present in only one or the other of the variables. This is clearly not true for our case. A general solution of the least squares problem is available (see, for instance, *York* [1966, 1967]), but to take advantage of it we must first estimate the relative magnitudes of the random errors in TRM and NRM.

There are a variety of causes of the scatter of the points about the NRM-TRM segment. Uncertainties in measurement of remanent magnetization arise primarily from scale reading errors and drift of the magnetometer calibration with time. Except for unusually low magnetizations, the uncertainty is roughly proportional to the remanence and is quite small (a few tenths of a percent). Frequently, however, the scatter is much greater than can be accounted for by these uncertainties in measurement; thus other factors are suggested such as failure to reproduce the temperature exactly in the pairs of heating steps or imperfect coincidence of the NRM and TRM

spectra. Such differences in remanence spectra would cause us to reject the NRM-TRM segment if they were large and systematic, but small fluctuating changes in magnetic properties may be caused by variations in local oxygen fugacity in the rock due to partial self-buffering. The relative contribution of such effects to error in NRM and TRM while the Thelliers' method is being used with a given rock is very complicated in detail, but a reasonable approximation overall may be that the errors in each are proportional to the fields that produced the remanence and to the rate of change of remanence with temperature at each point. The rate of change, however, is highly variable from rock to rock and hence cannot be used to make any simple generalizations about the structure of errors.

Let us assume, then, that to a very crude approximation the variances of TRM (σ_x^2) and NRM (σ_y^2) about the ideal line are given at every temperature by $\sigma_x^2 = (F_L\sigma)^2$ and $\sigma_y^2 = (F_E\sigma)^2$, where σ is a constant independent of temperature. This takes into account our belief that the absolute errors in determining the remanence of a given rock specimen due to causes as discussed above will be larger when the field that produces that remanence (and thus the remanence itself) is larger. Although this assumption is surely a very crude generalization, it is better than assuming that all the error is in x or y alone, and it reduces to the intuitively reasonable special case that the errors in x and y are most likely to be equal when $F_L = F_E$. Moreover, it permits an extremely simple solution of the generalized least squares problem. Using relative weights $w_x = 1/\sigma_x^2$ and $w_x = 1/\sigma_y^2$ for the sum of the squares of the x and y residuals to be minimized and the result from the theory of the Thelliers' method (equation (1)) that the ideal slope $b = -F_E/F_L$, we obtain by following the treatment of *York* [1966, 1967] a least squares slope

$$b = -\left[\sum_i (y_i - \bar{y})^2 \Big/ \sum_i (x_i - \bar{x})^2 \right]^{1/2} \qquad (2)$$

and standard error of the slope

$$\sigma_b = \left[\frac{2 \sum_i (y_i - \bar{y})^2 - 2b \sum_i (x_i - \bar{x})(y_i - \bar{y})}{(N-2) \sum_i (x_i - \bar{x})^2} \right]^{1/2} \qquad (3)$$

where $\bar{x}$ and $\bar{y}$ are ordinary (unweighted) arithmetic means. For plotting the line the y intercept (y_T in Figure 2) is simply $a = \bar{y} - b\bar{x}$. The geometry of adjustment of individual points is shown in Figure 7.

These formulae are more nearly correct than and equally as convenient as those for the usual single-variable linear regression. Compared with the much more complicated exact solution, which would weight each point differently and would require iterative numerical methods, this solution commonly underemphasizes the points near both ends of the line, where the remanence is usually changing very slowly with temperature. When the scatter is so low that errors in measurement of remanence dominate, any least squares method of estimating the slope is probably sufficiently accurate. If the experiment is arranged so that F_L is approximately the same as F_E, the relative errors in NRM and TRM are likely to conform more nearly to our simple assumption from which (2) and (3) are derived. In summary, we believe that the slope calculated by (2) is quite accurate enough for the usual sets of data in paleointensity work but that the standard error of the slope given by (3) cannot be attributed strict statistical meaning and must instead be regarded as an ad hoc measure of uncertainty.

We now turn to the question of the overall quality of an individual paleointensity determination. Even for specimens within a single flow the range in quality is often large. We need to construct a meaningful index of quality that can serve for comparative purposes and provide the basis for weighting individual determinations when we are computing the mean paleointensity for a lava flow.

One factor relating to the quality is surely the uncertainty in slope caused by the scatter of points about the least squares line. For comparison between flows the appropriate quantity is $\sigma_b/|b|$ because this is independent of the choice of laboratory field and is an expression of the relative uncertainty in F_E. This may be seen as follows: $F_E = F_L|b|$ (equation (1)), so $\sigma_F = F_L\sigma_b$, and the relative uncertainty in F_E, $\sigma_F/F_E = (F_L/F_E)\sigma_b = \sigma_b/|b|$.

There are two other factors that we believe must enter into the assessment of quality. These deal with the possibility that significant systematic errors in the slope may exist. Clearly, this possibility increases as the thoroughness of testing of the NRM decreases, i.e., as the fraction of NRM spanned by the acceptable NRM-TRM segment decreases and as the gaps in NRM between points along the segment increase. We may express this in terms of two factors or figures of merit that vary from 0 to 1 as the degree of coverage of NRM varies from low to high: (1) NRM fraction f, $f = \Delta y_T/y_T$; that is, it is the fraction of the total extrapolated NRM spanned by the chosen segment of the NRM-TRM curve (Figure 7). (2) Gap factor g, $g = 1 - \bar{\Delta}\bar{y}/\Delta y_T$, where Δy_T is the length of the NRM-TRM segment and $\bar{\Delta}\bar{y} = (1/\Delta y_T)\sum_{i=1}^{N-1} \Delta y_i^2$ is a weighted mean of the gaps Δy_i between the N points along the segment (Figure 7). For 2, 3, 4, $\cdots$, N evenly spaced points, $g = 0, \frac{1}{2}, \frac{2}{3}, \cdots, (N-2)/(N-1)$; and for a given number of points, g decreases as the spacing becomes less uniform.

These factors combined with the relative uncertainty in slope $\sigma_b/|b|$ provide our index of quality: $q = |b|\, fg/\sigma_b$. Note that σ_b is not independent of f and g. In the case of the size and distribution of gaps between points the effects on q differ: for a given degree of scatter of points from the least squares line, σ_b is reduced if the points are concentrated toward both ends of the line, whereas g is maximized if the points are distributed evenly along the line. In the case of the NRM fraction, however, the lower the value of f for a given number of points and degree of scatter, the higher the value of σ_b. Thus q depends doubly on f, as can be seen from our data in Table 2, for which q is roughly proportional to f^2. Nonetheless, given the difficulty of picking the correct short line segment from nonideal NRM-TRM data and the increased dangers of unrecognized systematic errors, we believe that this strong dependence of quality on NRM fraction is justified.

The reciprocal of q is an estimate of the relative uncertainty of a single paleointensity determination, although it cannot be given a strict probabilistic meaning. In analogy to the usual procedure of weighting according to the reciprocal of variance we use $w_j = 1/\sigma_F^2 = (q_j/F_{Ej})^2$ to compute the weighted mean paleointensity of a flow, $\bar{F}_E$. From this,

$$\bar{F}_E = \sum_j w_j F_{Ej} \Big/ \sum_j w_j \qquad (4)$$

where F_{Ej} is the paleointensity estimate and w_j is the weighting factor for each specimen in the flow.

To estimate the uncertainty of the mean we use the standard expression

$$\sigma_{\bar{F}} = \left\{ \left[\sum_j (F_{Ej} - \bar{F}_E)^2 \right] \Big/ N(N-1) \right\}^{1/2} \qquad (5)$$

where, however, $\bar{F}_E$ is the weighted mean. This is the most conservative measure because it assigns equal weight to each residual regardless of the quality of F_{Ej}. If $1/w_j$ were a statistically valid estimate of the variance of the F_{Ej}, then the best estimate of the standard error of $\bar{F}_E$ would be $(\sum_j w_j)^{-1/2}$. With our values of w_j the standard errors calculated this way are on the average about half as large as those calculated according to (5).

Acknowledgments. Many discussions with Richard R. Doell, Allan Cox, and G. Brent Dalrymple over the past 10 years have greatly stimulated our thinking, and we thank Richard Doell and Peter J. Smith for providing unpublished data. Discussions with Václav Bucha, M. F. Barbetti, M. W. McElhinny, and Stephen C. Robinson were very helpful, as were the reviews of Allan Cox, R. T. Merrill, and M. Prévot. R. S. C. gratefully acknowledges support by the U.S. National Academy of Sciences and the Czechoslovakian Academy of Sciences as an exchange scientist and by the Australian National University as a visiting research fellow during various stages in the preparation of the manuscript. We thank Rodd J. May, Abdulwahab A. Khodair, and Monte Marshall for assisting in the field work and Howard A. Powers for guidance in the field during an earlier expedition.

REFERENCES

Alldredge, L. R., and L. Hurwitz, Radial dipoles as the source of the earth's main magnetic field, *J. Geophys. Res., 69,* 2631–2640, 1964.

Arai, Y., Secular variation in the intensity of the past geomagnetic field, M.S. thesis, 84 pp., Univ. of Tokyo, Tokyo, Japan, 1963.

Aziz-ur-Rahman and I. McDougall, Paleomagnetism and paleosecular variation on lavas from Norfolk and Philip Islands, southwest Pacific Ocean, *Geophys. J. Roy. Astron. Soc., 33,* 141–155, 1973.

Bingham, D. K., and D. B. Stone, Paleosecular variation of the geomagnetic field in the Aleutian Islands, Alaska, *Geophys. J. Roy. Astron. Soc., 28,* 317–335, 1972.

Bucha, V., Influence of the earth's magnetic field on radiocarbon dating, in *Radiocarbon Variations and Absolute Chronology,* edited by I. U. Olsson, John Wiley, New York, 1970.

Bucha, V., Archaeomagnetic dating, in *Dating Techniques for the Archaeologist,* edited by H. N. Michael and E. K. Ralph, MIT Press, Cambridge, Mass., 1971.

Bullard, E. C., C. Freedman, H. Gellman, and J. Nixon, The westward drift of the earth's magnetic field, *Phil. Trans. Roy. Soc. London, Ser. A, 243,* 67–92, 1950.

Coe, R. S., Paleointensities of the earth's magnetic field determined from Tertiary and Quaternary rocks, *J. Geophys. Res., 72,* 3247–3262, 1967*a*.

Coe, R. S., The determination of paleo-intensities of the earth's magnetic field with emphasis on mechanisms which could cause nonideal behavior in Thelliers' method, *J. Geomagn. Geoelec., 19,* 157–179, 1967*b*.

Coe, R. S., Source models to account for Lake Mungo paleomagnetic excursion and their implications, *Nature, 269,* 49–51, 1977.

Coe, R. S., and C. S. Grommé, A comparison of three methods of determining geomagnetic paleointensities, *J. Geomagn. Geoelec., 25,* 415–435, 1973.

Cox, A., Lengths of geomagnetic polarity intervals, *J. Geophys. Res., 73,* 3247–3260, 1968.

Cox, A., Confidence limits for the precision parameter *K, Geophys. J. Roy. Astron. Soc., 18,* 545–549, 1969.

Cox, A., Latitude dependence of the angular dispersion of the geomagnetic field, *Geophys. J. Roy. Astron. Soc., 20,* 253–269, 1970.

Cox, A., The frequency of geomagnetic reversals and the symmetry of the nondipole field, *Rev. Geophys. Space Phys., 13,* 35–51, 1975.

Cox, A., and J. C. Cain, International conference on the core-mantle interface, *Eos Trans. AGU, 53,* 591–597, 1972.

Cox, A., and R. R. Doell, Long period variations of the geomagnetic field, *Bull. Seismol. Soc. Amer., 54,* 2243–2270, 1964.

Creer, K. M., Geomagnetic secular variations during the last 25,000 years: An interpretation of data obtained from rapidly deposited sediments, *Geophys. J. Roy. Astron. Soc., 48,* 91–109, 1977.

Damon, P. E., Climatic versus magnetic perturbation of the atmospheric C-14 reservoir, in *Radiocarbon Variations and Absolute Chronology,* edited by I. U. Olsson, John Wiley, New York, 1970.

Damon, P. E., A. Long, and E. I. Wallick, Dendrochronologic calibration of the carbon-14 time scale, in *Proceedings of the 8th International Conference on Radiocarbon Dating,* edited by T. A. Rafter and T. Grant-Taylor, Royal Society of New Zealand, Wellington, New Zealand, 1972.

Doell, R. R., Paleomagnetism of the Kau volcanic series, Hawaii, *J. Geophys. Res., 74,* 4857–4868, 1969.

Doell, R. R., Paleomagnetism of lava flows from Kauai, Hawaii, *J. Geophys. Res., 77,* 862–876, 1972*a*.

Doell, R. R., Paleosecular variation of the Honolulu volcanic series, Oahu, Hawaii, *J. Geophys. Res., 77,* 2129–2138, 1972*b*.

Doell, R. R., Paleomagnetism of volcanic rocks from Niihau, Nihoa, and Necker Islands, Hawaii, *J. Geophys. Res., 77,* 3725–3730, 1972*c*.

Doell, R. R., and A. Cox, The accuracy of the paleomagnetic method as evaluated from historic Hawaiian lava flows, *J. Geophys. Res., 68,* 1997–2009, 1963.

Doell, R. R., and A. Cox, Paleomagnetism of Hawaiian lava flows, *J. Geophys. Res., 70,* 3377–3405, 1965.

Doell, R. R., and A. Cox, Pacific geomagnetic secular variation, *Science, 171,* 248–254, 1971.

Doell. R. R., and A. Cox, The Pacific geomagnetic secular variation anomaly and the question of lateral uniformity in the lower mantle, in *The Nature of the Solid Earth,* edited by E. C. Robertson, McGraw-Hill, New York, 1972.

Doell, R. R., and G. B. Dalrymple, Potassium-argon ages and paleomagnetism of the Waianae and Koolau volcanic series, Oahu, Hawaii, *Bull. Geol. Soc. Amer., 84,* 1217–1242, 1973.

Doell, R. R., and P. J. Smith, On the use of magnetic cleaning in paleointensity studies, *J. Geomagn. Geoelec., 21,* 579–594, 1969.

Duncan, R. A., Palaeosecular variation at the Society Islands. French Polynesia, *Geophys. J. Roy. Astron. Soc., 41,* 245–254, 1975.

Fisher, R. A., Dispersion on a sphere, *Proc. Roy. Soc., Ser. A, 217,* 295–305, 1953.

Isaacson, L. B., and D. F. Heinrichs, Paleomagnetism and secular variation of Easter Island basalts, *J. Geophys. Res., 81,* 1476–1482, 1976.

Khodair, A. A., and R. S. Coe, Determination of geomagnetic paleointensities in vacuum, *Geophys. J. Roy. Astron. Soc., 42,* 107–115, 1975.

Kono, M., Intensity of the earth's magnetic field during the Pliocene and Pleistocene in relation to the amplitude of mid-ocean ridge magnetic anomalies, *Earth Planet. Sci. Lett., 11,* 10–17, 1971.

Lingenfelter, R. E., and R. Ramaty, Astrophysical and geophysical variations in C-14 production, in *Radiocarbon Variation and Absolute Chronology,* edited by I. U. Olsson, John Wiley, New York, 1970.

McDonald, K. L., and R. H. Gunst, An analysis of the Earth's magnetic field from 1855 to 1965, *Tech. Rep. IER-46-IES-1,* Nat. Oceanic and Atmos. Admin., Boulder, Colo., 1967.

McElhinny, M. W., and R. T. Merrill, Geomagnetic secular variation over the past 5 m.y., *Rev. Geophys. Space Phys., 13,* 687–708, 1975.

Nagata, T., Y. Arai, and K. Momose, Secular variation of the geomagnetic total force during the last 5000 years, *J. Geophys. Res., 68,* 5277–5281, 1963.

Ozima, M., and Y. Aoki, Quiet secular variation in Japan during the last 9500 years, *J. Geomagn. Geoelec., 24,* 471–477, 1972.

Ozima, M., and M. Ozima, Characteristic thermomagnetic curve in submarine basalts, *J. Geophys. Res., 76,* 2051–2056, 1971.

Porter, S. C., Holocene eruptions of Mauna Kea volcano, Hawaii, *Science, 172,* 375–377, 1971.

Powers, H. A., A chronology of the explosive eruptions of Kilauea, *Pac. Sci., 2,* 278–292, 1948.

Powers, H. A., A new date in Kilauea's history, *Volcano Lett., 527,* 3, 1955.

Rubin, M., and C. Alexander, U.S. Geological Survey radiocarbon dates, V, *Radiocarbon, 2,* 129–185, 1960.

Rubin, M., and S. M. Berthold, U.S. Geological Survey radiocarbon dates, VI, *Radiocarbon, 3,* 86–98, 1961.

Rubin, M., and H. E. Suess, U.S. Geological Survey radiocarbon dates, III, *Science, 123,* 442–448, 1956.

Smith, P. J., The intensity of the ancient geomagnetic field: A review and analysis, *Geophys. J. Roy. Astron. Soc., 12,* 321–362, 1967.

Stacey, F. D., *Physics of the Earth,* 324 pp., John Wiley, New York, 1969.

Stearns, H. T., and G. A. MacDonald, Geology and groundwater resources of the Island of Hawaii, *Bull. Hawaii Div. Hydrogr., 9,* 363 pp., 1946.

Sullivan, B. M., E. Spiker, and M. Rubin, U.S. Geological Survey radiocarbon dates, XI, *Radiocarbon, 12,* 319–334, 1970.

Thellier, E., and O. Thellier, Sur l'intensité du champ magnétique terrestre dans le passé historique et géologique, *Ann. Geophys., 15,* 285–376, 1959.

Vestine, E. H., L. Laporte, I. Lange, and W. E. Scott, The geomagnetic field, its description and analysis, *Carnegie Inst. Wash. Publ., 580,* 1947*a*.

Vestine, E. H., L. Laporte, C. Cooper, I. Lange, and W. C. Hendrix, Description of the Earth's main magnetic field and its secular change, 1905–1945, *Carnegie Inst. Wash. Publ., 578,* 1947*b*.

Wilson, R. L., Paleomagnetism in northern Ireland, I, The thermal demagnetization of natural magnetic moments in rocks, *Geophys. J. Roy. Astron. Soc., 5,* 45–58, 1961.

Wilson, R. L., Permanent aspects of the earth's non-dipole magnetic field over upper Tertiary times, *Geophys. J. Roy. Astron. Soc., 19,* 417–437, 1970.

Wilson, R. L., Dipole offset—The time-average paleomagnetic field over the past 25 million years, *Geophys. J. Roy. Astron. Soc., 22,* 491–504, 1971.

Wilson, R. L., Paleomagnetic differences between normal and reversed field sources, and the problem of far-sided and right-handed pole positions, *Geophys. J. Roy. Astron. Soc., 28,* 295–304, 1972.

York, D., Least-squares fitting of a straight line, *Can. J. Phys., 44,* 1079–1086, 1966.

York, D., The best isochron, *Earth Planet. Sci. Lett., 2,* 479–482, 1967.

Yukutake, T., and H. Tachinaka, The non-dipole part of the earth's magnetic field, *Bull. Earthquake Res. Inst. Tokyo Univ., 46,* 1027–1074, 1968.

Yukutake, T., and H. Tachinaka, Separation of the earth's magnetic field into the drifting and standing parts, *Bull. Earthquake Res. Inst. Tokyo Univ., 47,* 65–97, 1969.

(Received May 1, 1977;
revised November 16, 1977;
accepted November 28, 1977.)